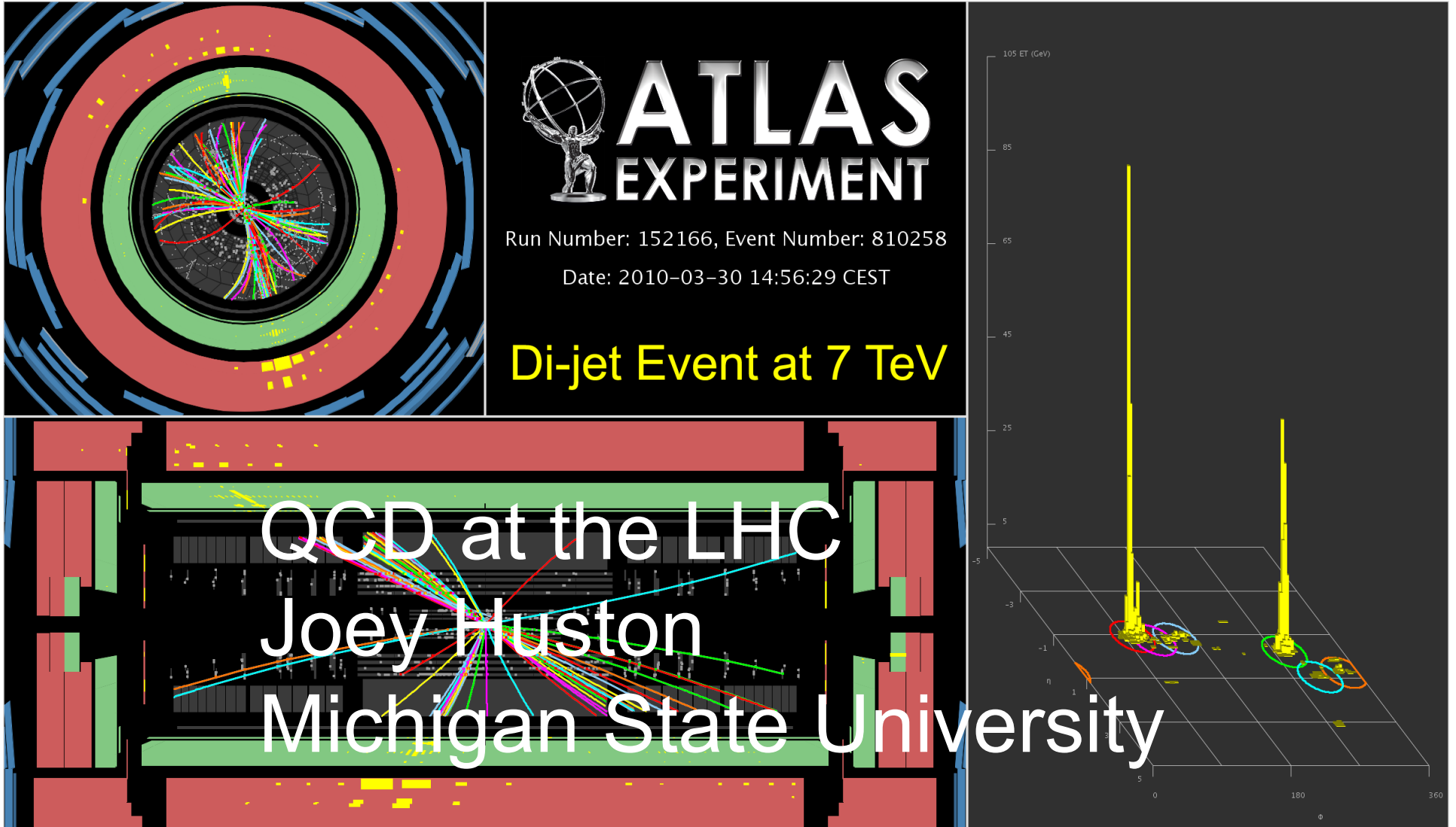


Lecture 2



NLO calculations

- NLO calculation requires consideration of all diagrams that have an extra factor of α_s
 - ◆ real radiation, as we have just discussed
 - ◆ virtual diagrams (with loops)
- For virtual diagram, have to integrate over loop momentum
 - ◆ but result contains IR singularities (soft and collinear), just as found for tree-level diagrams

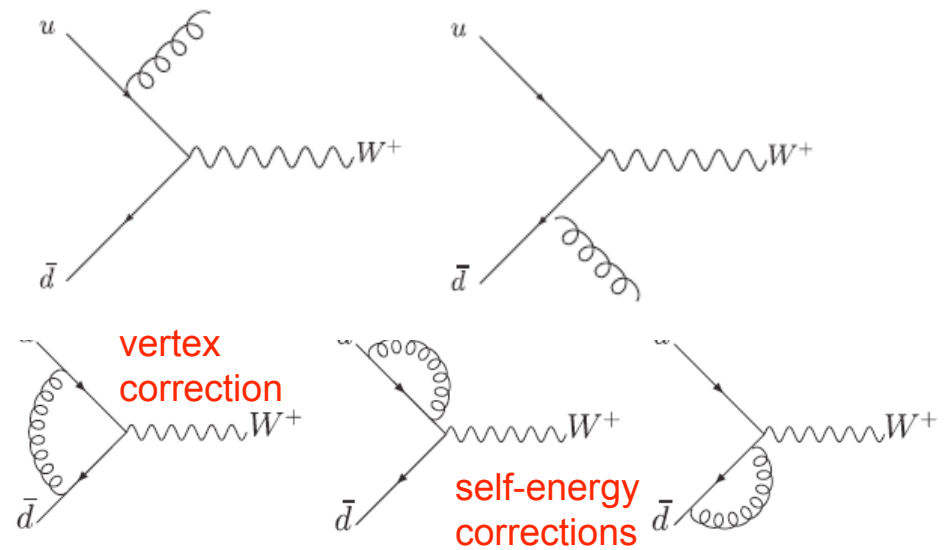


Figure 14. Virtual diagrams included in the next-to-leading order corrections to the Drell-Yan production of a W at hadron colliders.

$O(\alpha_s)$ virtual corrections in NLO cross section arise from interference between tree level and one-loop virtual amplitudes

If we add the real+virtual contributions, we find that the singularities will cancel, for inclusive cross sections. We have to be more clever for differential distributions.

Advantages of NLO

- Less sensitivity to unphysical input scales, i.e. renormalization and factorization scales
- First level of prediction where normalization (and sometimes shape) can be taken seriously
- More physics
 - ♦ parton merging gives structure in jets
 - ♦ initial state radiation
 - ♦ more species of incoming partons
- Suppose I have a cross section σ calculated to NLO ($O(\alpha_s^n)$)
- Any remaining scale dependence is of one order higher ($O(\alpha_s^{n+1})$)
 - ♦ in fact, we know the scale dependent part of the $O(\alpha_s^{n+1})$ cross section before we perform the complete calculation, since the scale-dependent terms are explicit at the previous order

$$\begin{aligned} \frac{d\sigma}{dE_T} = & \alpha_s(\mu_R)^2 \textcolor{green}{A} \quad \text{Inclusive jet prod at NNLO} \\ & + \alpha_s(\mu_R)^3 (\textcolor{blue}{B} + 2b_0 L \textcolor{green}{A}) \\ & + \alpha_s(\mu_R)^4 (\textcolor{red}{C} + 3b_0 L \textcolor{blue}{B} + (3b_0^2 L^2 + 2b_1 L) \textcolor{green}{A}) \end{aligned}$$

with $L = \log(\mu_R/E_T)$ and b_i the known beta function coefficients.

we know A and B, not C

Renormalisation scale dependence

LO has monotonic scale dependence

non-monotonic at NLO

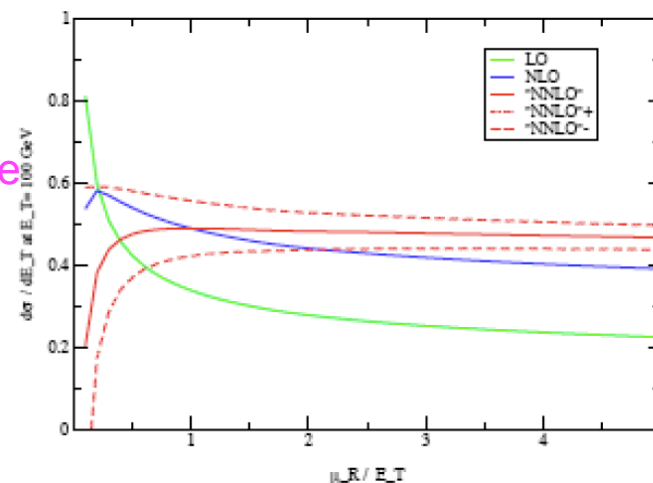


Figure 11: Single jet inclusive distribution at $E_T = 100$ GeV and $0.1 < |\eta| < 0.7$ at $\sqrt{s} = 1800$

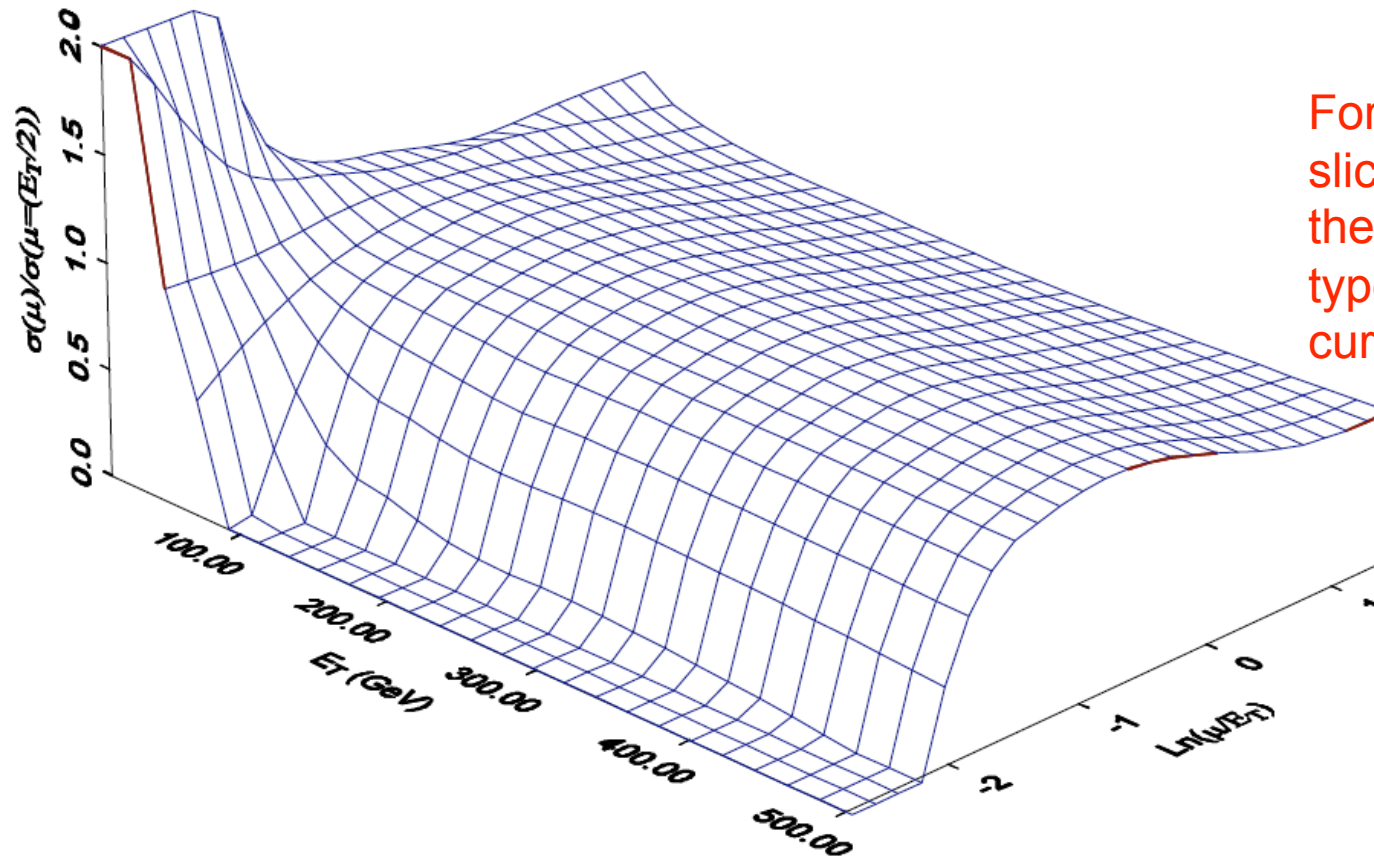
The NNLO coefficient $\textcolor{red}{C}$ is unknown. The curves show the guesses $C = 0$ (solid) and $C = \pm B^2/A$ (dashed).

Predictions tend to be more reliable at higher E_T

SDEodfmuf Mar. 20, 1997 7:43:09 AM

μ Dependence of Inclusive Jet Cross Section
 $\sqrt{s} = 1800 \text{ GeV}, 0.1 < \eta < 0.7, \text{HMRS(B),ppbar}$

$R=0.7$



For fixed fixed E_T
slices, note
the parabolic
type shape for the
curve

Back to W production to NLO

- In 4-dimensions, the contribution of the real diagrams can be written (ignoring diagrams with incoming gluons for simplicity)

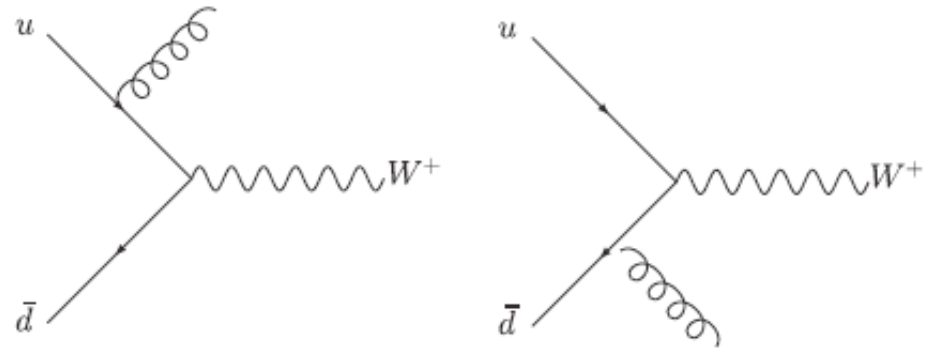
$$|M(u\bar{d} \rightarrow W^+ g)|^2 \sim g^2 C_F \left[\frac{\hat{u}}{\hat{t}} + \frac{\hat{t}}{\hat{u}} + \frac{2Q^2 \hat{s}}{\hat{u}\hat{t}} \right]$$

$$\sim g^2 C_F \left[\left(\frac{1+z^2}{1-z} \right) \left(\frac{-\hat{s}}{\hat{t}} + \frac{-\hat{s}}{\hat{u}} \right) - 2 \right]$$

♦ where

$$z = \frac{Q^2}{s} \text{ and } \hat{s} + \hat{t} + \hat{u} = Q^2$$

- Note that the real diagrams contain collinear singularities, $u \rightarrow 0$, $t \rightarrow 0$, and soft singularities, $z \rightarrow 1$



...thanks to Keith Ellis for the next few slides

and don't sweat the details; I just want you to see in general terms how a NLO calculation is carried out

Aside: dimensional regularization

- Suppose we have an integral of the form, typical of the integrals in a NLO calculation

$$I = \int \frac{d^4 k}{(2\pi)^4} \frac{1}{(k^2 - m^2)^2}$$

- We get infinity if we integrate this in 4 dimensions, so go to $4-2\varepsilon$ dimensions

$$\int \frac{d^4 k}{(2\pi)^4} \rightarrow (\mu)^{2\varepsilon} \int \frac{d^{4-2\varepsilon} k}{(2\pi)^{4-2\varepsilon}} \rightarrow (\mu)^{2\varepsilon} \int \frac{d\Omega_{4-2\varepsilon}}{(2\pi)^{4-2\varepsilon}} \int dk_E k_E^{3-2\varepsilon}$$

$$\int \frac{d\Omega_{4-2\varepsilon}}{(2\pi)^{4-2\varepsilon}} = \frac{2}{(4\pi)^{2-\varepsilon}} \frac{1}{\Gamma(2-\varepsilon)}$$

$$(\mu)^{2\varepsilon} \int_0^\infty dk_E \frac{k_E^{3-2\varepsilon}}{(k_E^2 + m^2)^2} = \frac{(\mu)^{2\varepsilon}}{2(m)^{2\varepsilon}} \int_0^1 dz z^{1-\varepsilon} (1-z)^{\varepsilon-1} = \frac{1}{2} \left(\frac{\mu}{m} \right)^{2\varepsilon} \frac{\Gamma(\varepsilon)\Gamma(2-\varepsilon)}{\Gamma(2)}$$

- Using

$$\Gamma(1+z) = z\Gamma(z); \Gamma'(1) = -\gamma_E = -0.5772\dots$$

Dimensional regularization, continued

- Find

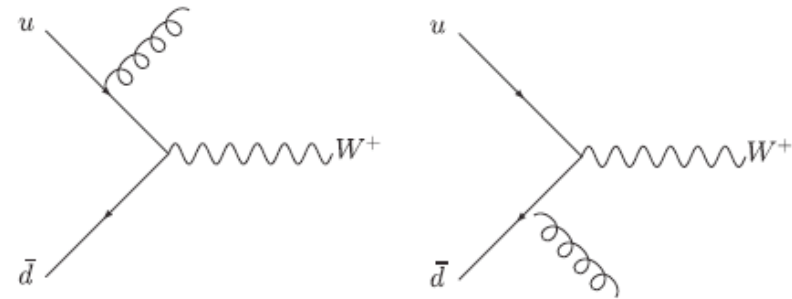
$$I = \frac{\Gamma(\varepsilon)}{(4\pi)^{2-\varepsilon}} \left(\frac{\mu}{m}\right)^{2\varepsilon} \xrightarrow{\varepsilon \rightarrow 0} \frac{1}{(4\pi)^2} \left[+\frac{1}{\varepsilon} - \gamma_E + \ln(4\pi) + 2\ln\left(\frac{\mu}{m}\right) + O(\varepsilon) \right]$$

- ♦ singular bits, plus finite bits as $\varepsilon \rightarrow 0$, plus log singularity as $m \rightarrow 0$

- Define $\overline{\text{MS}}$ scheme: subtract (absorb) $1/\varepsilon$ pole, γ_E , and $\ln(4\pi)$ bits

Now do the dimension trick for the real part

- Problem: if I work in 4 dimensions, I get divergences
- Solution: working in $4-2\epsilon$ dimensions, to control the divergences (dimensional reduction)



$$\sigma_{real} = \frac{\alpha_s}{2\pi} C_F \left(\frac{\mu^2}{Q^2} \right)^\epsilon c_\Gamma \left[\left(\frac{2}{\epsilon^2} + \frac{3}{\epsilon} - \frac{\pi^2}{3} \right) \delta(1-z) - \frac{2}{\epsilon} P_{qq}(z) - 2(1-z) + 4(1+z^2) \left[\frac{\ln(1-z)}{1-z} \right]_+ - 2 \frac{1+z^2}{1-z} \ln z \right]$$

- with

$$c_\Gamma = \frac{(4\pi)^\epsilon}{\Gamma(1-\epsilon)}$$

$$\left(\frac{\log(1-z)}{1-z} \right)_+ \equiv \lim_{\beta \rightarrow 0} \left\{ \frac{\log(1-z)}{1-z} \theta(1-z-\beta) + \frac{1}{2} \log^2(\beta) \delta(1-z-\beta) \right\}$$

“+ distribution”

We get $1/\epsilon$ terms from individual soft and collinear singularities
 We get $1/\epsilon^2$ terms for overlapping IR singularities.

Ditto for the virtual part

$$\sigma_{virt} = \delta(1-z) \left[1 + \frac{\alpha_s}{2\pi} C_F \left(\frac{\mu^2}{Q^2} \right)^\epsilon c'_\Gamma \left(-\frac{2}{\epsilon^2} - \frac{3}{\epsilon} - 6 + \pi^2 \right) \right] \quad \text{from soft and collinear bits}$$

• where

$$c'_\Gamma = c_\Gamma + \mathcal{O}(\epsilon^3)$$

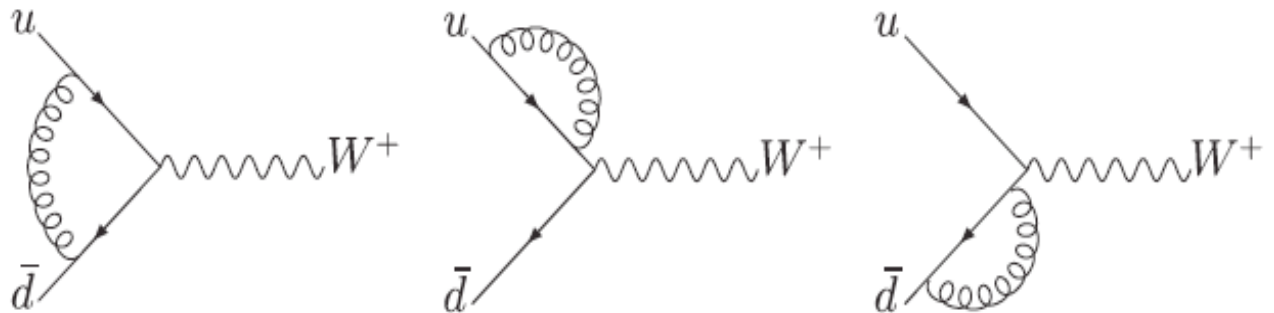


Figure 14. Virtual diagrams included in the next-to-leading order corrections to the Drell–Yan production of a W at hadron colliders.

We also get UV divergences when the loop momenta go off to infinity. The summation of these singularities leads to the running of the strong couplings, i.e. we define the sum of all such contributions (scales $> \mu_{UV}$) as the physical renormalized coupling, α_s .

Now add real and virtual

$$\sigma_{real+virt} = \frac{\alpha_s}{2\pi} C_F \left(\frac{\mu^2}{Q^2} \right)^\epsilon c_\Gamma \left[\left(\frac{2\pi^2}{3} - 6 \right) \delta(1-z) - \frac{2}{\epsilon} P_{qq}(z) - 2(1-z) + 4(1+z^2) \left[\frac{\ln(1-z)}{1-z} \right]_+ - 2 \frac{1+z^2}{1-z} \ln z \right]$$

- Notice that the ϵ^2 terms cancel
- The divergences that are proportional to the branching probabilities are universal
- We can factorize them into the parton distributions, performing mass factorization by subtracting the counter-term (MSbar scheme)

$$2 \frac{\alpha_s}{2\pi} C_F \left[\frac{-c_\Gamma}{\epsilon} P_{qq}(z) - (1-z) + \delta(1-z) \right]$$

- To get

$$\hat{\sigma}_{real+virt} = \frac{\alpha_s}{2\pi} C_F \left[\left(\frac{2\pi^2}{3} - 8 \right) \delta(1-z) + 4(1+z^2) \left[\frac{\ln(1-z)}{1-z} \right]_+ - 2 \frac{1+z^2}{1-z} \ln z + 2 P_{qq}(z) \ln \frac{Q^2}{\mu^2} \right]$$

- Plus a similar correction for incoming gluons
- That works for the total cross section, but we need differential distributions for comparisons to data, so we need a general subtraction procedure at NLO, using Monte Carlo techniques

In general

- That works for the total cross section, but we need differential distributions for comparisons to data, so we need a general subtraction procedure at NLO, using Monte Carlo techniques
- For incoming partons a and b, producing m outgoing partons

$$\sigma_{ab} = \sigma_{ab}^{LO} + \sigma_{ab}^{NLO}$$

$$\sigma_{ab}^{LO} = \int_m d\sigma_{ab}^{Born}$$

$$\sigma_{ab}^{NLO} = \int_{m+1} d\sigma_{ab}^{real} + \int_m d\sigma_{ab}^{virt}$$

the singular parts of the matrix elements for real emission, corresponding to soft and collinear emission, can be isolated in a process independent manner; of course it gets a lot more complicated for large m

- We have to construct a series of counter-terms

$$d\sigma_{ct} = \sum_{ct} \int_m d\sigma_B \otimes \int_1 dV_{ct}$$

- Where σ_B denotes the appropriate color and spin projection of the Born level cross section, and the counter-terms are independent of the details of the process under consideration

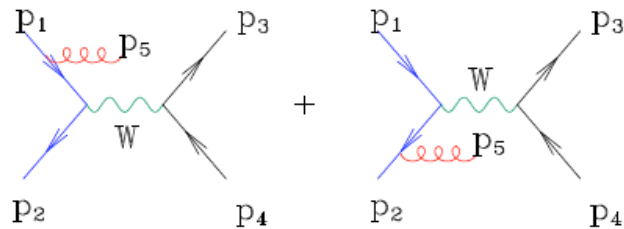
Catani-Seymour subtraction

- These counter-terms cancel all non-integrable singularities in $d\sigma^{\text{real}}$, so that one can write

$$\sigma_{ab}^{NLO} = \int_{m+1} \left[d\sigma_{ab}^{\text{real}} - d\sigma_{ab}^{\text{ct}} \right] + \int_{m+1} d\sigma_{ab}^{\text{ct}} + \int_m d\sigma_{ab}^{\text{virt}}$$

- The phase space integration in the first term can now be performed numerically in 4 dimensions
- The integral in the 2nd term can be done easily and analytically

Consider matrix element counter-event for W production



real corrections to W production
at NLO

- In soft limit ($p_5 \rightarrow 0$), we have

$$|M_1(p_1, p_2, p_3, p_4, p_5)|^2 = g^2 C_F \frac{p_1 \cdot p_2}{p_1 \cdot p_5 p_2 \cdot p_5} |M_0(p_1, p_2, p_3, p_4)|^2$$

eikonal factor; an approximation to the full matrix element valid when the gluon is soft

- The eikonal factor can be associated with radiation from a given leg by partial fractioning

$$\frac{p_1 \cdot p_2}{p_1 \cdot p_5 p_2 \cdot p_5} = \left[\frac{p_1 \cdot p_2}{p_1 \cdot p_5 + p_2 \cdot p_5} \right] \left[\frac{1}{p_1 \cdot p_5} + \frac{1}{p_2 \cdot p_5} \right]$$

These are the Catani-Seymour dipoles (actually single collinear poles produced by partial fractioning); Keith Ellis thinks Catani and Seymour should be shot for

- Including the collinear contributions, singular as $p_1 \cdot p_5 \rightarrow 0$, the matrix element for the counter-event has the structure

calling these dipoles; maybe we can take a vote

$$|M_1(p_1, p_2, p_3, p_4, p_5)|^2 = \frac{g^2}{x_a p_1 \cdot p_5} \hat{P}_{qq}(x_a) |M_0(p_1, p_2, p_3, p_4)|^2$$

- where

$$1 - x_a = \frac{p_1 \cdot p_5 + p_2 \cdot p_5}{p_1 \cdot p_2} \quad \hat{P}_{qq}(x_a) = C_F \frac{1 + x^2}{1 - x}$$

- Programs that do NLO calculations, such as MCFM, are parton-level Monte Carlo generators in which (weighted) events and counter-events are generated
 - ◆ for complicated processes, such as $W + 2$ jets, there can be many counter-events (24), corresponding to the Catani-Seymour subtraction terms, for each event
 - ◆ only the sum of all events (events + counter-events) is meaningful, since many positive and negative weights need to cancel against each other; if too few events are generated, or if the binning is too small, can have negative results
 - ◆ in general, cannot connect these complex NLO matrix elements to parton showering...although that's the dream/plan (see for example the Binoth Accord in the Les Houches 2009 writeup: arXiv:1003.1241)
 - ▲ processes such as $W, Z, WW, ZZ, \text{Higgs}, t\bar{t} \text{bar}, \text{single top}, \dots$ have been included in NLO parton shower Monte Carlo programs like MC@NLO, Powheg
 - MC@NLO $\sim 10\%$ negative weights; Powheg almost zero
 - ▲ state of the art now is $Z + 1$ jet (I believe)

Thomas Binoth 1965-2010

- This accord should make the kinds of discussion we're having here easier (in the future)
- Binoth Les Houches Accord

ABSTRACT: Many highly developed Monte Carlo tools for the evaluation of cross sections based on tree matrix elements exist and are used by experimental collaborations in high energy physics. As the evaluation of one-loop matrix elements has recently been undergoing enormous progress, the combination of one-loop matrix elements with existing Monte Carlo tools is on the horizon. This would lead to phenomenological predictions at the next-to-leading order level. This note summarises the discussion of the next-to-leading order multi-leg (NLM) working group on this issue which has been taking place during the workshop on Physics at TeV colliders at Les Houches, France, in June 2009. The result is a proposal for a standard interface between Monte Carlo tools and one-loop matrix element programs.

Dedicated to the memory of, and in tribute to, Thomas Binoth, who led the effort to develop this proposal for Les Houches 2009. Thomas led the discussions, set up the subgroups, collected the contributions, and wrote and edited this paper. He made a promise that the paper would be on the arXiv the first week of January, and we are faithfully fulfilling his promise. In his honor, we would like to call this the Binoth Les Houches Accord. The body of the paper is unchanged from the last version that can be found on his webpage http://www.ph.ed.ac.uk/~binoth/NLOLHA_CURRENT_VERSION.pdf

arXiv:1001.1307v1 [hep-ph] 8 Jan 2010

Preprint typeset in JHEP style - PAPER VERSION

A proposal for a standard interface between Monte Carlo tools and one-loop programs

T. Binoth

The University of Edinburgh, Edinburgh EH9 3JZ, Scotland

F. Boudjema *

LAPTH, 9 Chemin de Bellevue BP 110, 74941 Annecy-le-

G. Dissertori and A. Lazopoulos

Department of Physics, ETH Zurich, CH-8093 Zurich, Sw

A. Denner

Paul Scherrer Institut, Würenlingen und Villigen, CH-523

S. Dittmaier

Albert-Ludwigs-Universität Freiburg, Physikalisches Institut

R. Frederix, N. Greiner and S. Höche

University of Zurich, Winterthurerstrasse 190, CH-8057 Zurich, Switzerland

W. Giele, P. Skands and J. Winter

FNAL, P.O. Box 500, Batavia, IL 60510, USA

T. Gleisberg

SLAC, Stanford University, Stanford, CA 94309 USA

J. Archibald, G. Heinrich, F. Krauss and D. Maître

IPPP, University of Durham, South Rd, Durham DH1 3LE, United Kingdom

M. Huber

Max-Planck-Institut für Physik (Werner-Heisenberg-Institut), D-80805 München, Germany

J. Huston

Michigan State University, East Lansing, MI 48840, USA

N. Kauer

Department of Physics, Royal Holloway, University of London, Egham TW20 0EX, UK



MCFM

- Many processes available at LO and NLO
 - ◆ note these are partonic level only
- Option for ROOT output (see later)
- mcfm.fnal.gov

$$p\bar{p} \rightarrow W^{\pm}/Z$$

$$p\bar{p} \rightarrow W^{\pm} + Z$$

$$p\bar{p} \rightarrow W^{\pm} + \gamma$$

$$p\bar{p} \rightarrow W^{\pm} + g^* (\rightarrow b\bar{b})$$

$$p\bar{p} \rightarrow W^{\pm}/Z + 1 \text{ jet}$$

$$p\bar{p}(gg) \rightarrow H$$

$$p\bar{p}(VV) \rightarrow H + 2 \text{ jets}$$

$$pp \rightarrow t + W$$

$$p\bar{p} \rightarrow W^+ + W^-$$

$$p\bar{p} \rightarrow Z + Z$$

$$p\bar{p} \rightarrow W^{\pm}/Z + H$$

$$p\bar{p} \rightarrow Z b\bar{b}$$

$$p\bar{p} \rightarrow W^{\pm}/Z + 2 \text{ jets}$$

$$p\bar{p}(gg) \rightarrow H + 1 \text{ jet} \text{ (2 jets now)}$$

$$p\bar{p} \rightarrow t + X$$

State of the art

Relative order	2->1	2->2	2->3	2->4	2-5	2->6
1	LO					
α_s	NLO	LO				
α_s^2	NNLO	NLO	LO			
α_s^3		NNLO	NLO	LO		
α_s^4				NLO	LO	
α_s^5						LO

- LO: well under control, even for multiparticle final states
- NLO: well understood for 2->1, 2->2 and 2->3; first calculations of 2->4 (W +3 jets, ttbb)
- NNLO: known for inclusive and exclusive 2->1 (i.e. Higgs, Drell-Yan); work on 2->2 (Higgs + 1 jet)

An experimenter's wishlist

Run II Monte Carlo Workshop

Single Boson	Diboson	Triboson	Heavy Flavour
$W+ \leq 5j$	$WW+ \leq 5j$	$WWW+ \leq 3j$	$t\bar{t}+ \leq 3j$
$W + b\bar{b} \leq 3j$	$W + b\bar{b}+ \leq 3j$	$WWW + b\bar{b}+ \leq 3j$	$t\bar{t} + \gamma+ \leq 2j$
$W + c\bar{c} \leq 3j$	$W + c\bar{c}+ \leq 3j$	$WWW + \gamma\gamma+ \leq 3j$	$t\bar{t} + W+ \leq 2j$
$Z+ \leq 5j$	$ZZ+ \leq 5j$	$Z\gamma\gamma+ \leq 3j$	$t\bar{t} + Z+ \leq 2j$
$Z + b\bar{b}+ \leq 3j$	$Z + b\bar{b}+ \leq 3j$	$ZZZ+ \leq 3j$	$t\bar{t} + H+ \leq 2j$
$Z + c\bar{c}+ \leq 3j$	$ZZ + c\bar{c}+ \leq 3j$	$WZZ+ \leq 3j$	$t\bar{b} \leq 2j$
$\gamma+ \leq 5j$	$\gamma\gamma+ \leq 5j$	$ZZZ+ \leq 3j$	$b\bar{b}+ \leq 3j$
$\gamma + b\bar{b} \leq 3j$	$\gamma\gamma + b\bar{b} \leq 3j$		single top
$\gamma + c\bar{c} \leq 3j$	$\gamma\gamma + c\bar{c} \leq 3j$		
	$WZ+ \leq 5j$		
	$WZ + b\bar{b} \leq 3j$		
	$WZ + c\bar{c} \leq 3j$		
	$W\gamma+ \leq 3j$		
	$Z\gamma+ \leq 3j$		

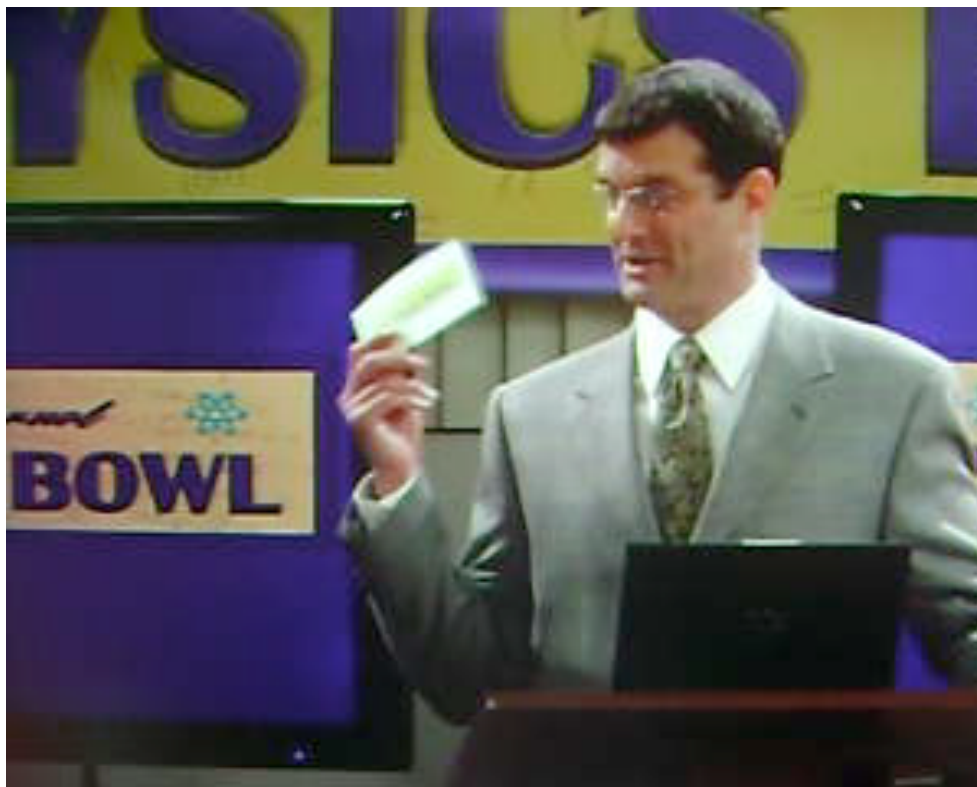
Realistic wishlist

- Was developed at Les Houches in 2005, and expanded in 2007 and 2009
- Calculations that are important for the LHC AND do-able in finite time
- In 2009, we added $t\bar{t}t$, $Wbbj$, $Z+3j$, $W+4j$ plus an extra column for each process indicating the level of precision required by the experiments
 - ◆ to see for example if EW corrections may need to be calculated
- In order to be most useful, decays for final state particles (t, W, H) need to be provided in the codes as well
- Since the publication of Les Houches 2009 in March, processes 6 and 7 have been completed
- $V + 4$ jets (process 10) is on the horizon

Process ($V \in \{Z, W, \gamma\}$)	Comments
Calculations completed since Les Houches 2005	
1. $pp \rightarrow VV\text{jet}$	$WW\text{jet}$ completed by Dittmaier/Kallweit/Uwer [4, 5]; Campbell/Ellis/Zanderighi [6]. $ZZ\text{jet}$ completed by Binoth/Gleisberg/Karg/Kauer/Sanguinetti [7]
2. $pp \rightarrow \text{Higgs}+2\text{jets}$	NLO QCD to the gg channel completed by Campbell/Ellis/Zanderighi [8]; NLO QCD+EW to the VBF channel completed by Ciccolini/Denner/Dittmaier [9, 10]
3. $pp \rightarrow VVV$	ZZZ completed by Lazopoulos/Melnikov/Petriello [11] and WWZ by Hankele/Zeppenfeld [12] (see also Binoth/Ossola/Papadopoulos/Pittau [13])
4. $pp \rightarrow t\bar{t}b\bar{b}$	relevant for $t\bar{t}H$ computed by Bredenstein/Denner/Dittmaier/Pozzorini [14, 15] and Bevilacqua/Czakon/Papadopoulos/Pittau/Worek [16]
5. $pp \rightarrow V+3\text{jets}$	calculated by the Blackhat/Sherpa [17] and Rocket [18] collaborations
Calculations remaining from Les Houches 2005	
6. $pp \rightarrow t\bar{t}+2\text{jets}$	relevant for $t\bar{t}H$ computed by Bevilacqua/Czakon/Papadopoulos/Worek [19]
7. $pp \rightarrow VVb\bar{b}$, 8. $pp \rightarrow VV+2\text{jets}$	relevant for $VBF \rightarrow H \rightarrow VV$, $t\bar{t}H$ relevant for $VBF \rightarrow H \rightarrow VV$ VBF contributions calculated by (Bozzi/Jäger/Oleari/Zeppenfeld [20–22])
NLO calculations added to list in 2007	
9. $pp \rightarrow b\bar{b}b\bar{b}$	$q\bar{q}$ channel calculated by Golem collaboration [23]
NLO calculations added to list in 2009	
10. $pp \rightarrow V+4\text{ jets}$ 11. $pp \rightarrow Wb\bar{b}j$ 12. $pp \rightarrow t\bar{t}t$	top pair production, various new physics signatures top, new physics signatures various new physics signatures
Calculations beyond NLO added in 2007	
13. $gg \rightarrow W^*W^* \mathcal{O}(\alpha^2\alpha_s^3)$ 14. NNLO $pp \rightarrow t\bar{t}$ 15. NNLO to VBF and $Z/\gamma+\text{jet}$	backgrounds to Higgs normalization of a benchmark process Higgs couplings and SM benchmark
Calculations including electroweak effects	
16. NNLO QCD+NLO EW for W/Z	precision calculation of a SM benchmark

Table 1: The updated experimenter's wishlist for LHC processes

If all else fails...

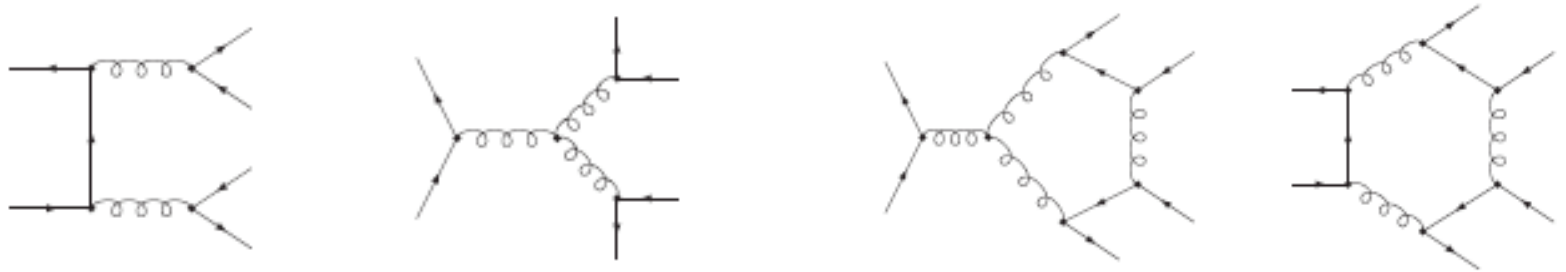


Process ($V \in \{Z, W, \gamma\}$)	Comments
Calculations completed since Les Houches 2005	
1. $pp \rightarrow VV\text{jet}$	$WW\text{jet}$ completed by Dittmaier/Kallweit/Uwer [4, 5]; Campbell/Ellis/Zanderighi [6]. $ZZ\text{jet}$ completed by Binoth/Gleisberg/Karg/Kauer/Sanguinetti [7]
2. $pp \rightarrow \text{Higgs}+2\text{jets}$	NLO QCD to the gg channel completed by Campbell/Ellis/Zanderighi [8]; NLO QCD+EW to the VBF channel completed by Ciccolini/Denner/Dittmaier [9, 10]
3. $pp \rightarrow VVV$	ZZZ completed by Lazopoulos/Melnikov/Petriello [11] and WWZ by Hankele/Zeppenfeld [12] (see also Binoth/Ossola/Papadopoulos/Pittau [13])
4. $pp \rightarrow t\bar{t}b\bar{b}$	relevant for $t\bar{t}H$ computed by Bredenstein/Denner/Dittmaier/Pozzorini [14, 15] and Bevilacqua/Czakon/Papadopoulos/Pittau/Worek [16]
5. $pp \rightarrow V+3\text{jets}$	calculated by the Blackhat/Sherpa [17] and Rocket [18] collaborations
Calculations remaining from Les Houches 2005	
6. $pp \rightarrow t\bar{t}+2\text{jets}$	relevant for $t\bar{t}H$ computed by Bevilacqua/Czakon/Papadopoulos/Worek [19]
7. $pp \rightarrow VVb\bar{b}$, 8. $pp \rightarrow VV+2\text{jets}$	relevant for VBF $\rightarrow H \rightarrow VV$, $t\bar{t}H$ relevant for VBF $\rightarrow H \rightarrow VV$ VBF contributions calculated by (Bozzi/Jäger/Oleari/Zeppenfeld [20–22])
NLO calculations added to list in 2007	
9. $pp \rightarrow b\bar{b}b\bar{b}$	$q\bar{q}$ channel calculated by Golem collaboration [23]
NLO calculations added to list in 2009	
10. $pp \rightarrow V+4\text{jets}$ 11. $pp \rightarrow Wb\bar{b}j$ 12. $pp \rightarrow t\bar{t}t\bar{t}$	top pair production, various new physics signatures top, new physics signatures various new physics signatures
Calculations beyond NLO added in 2007	
13. $gg \rightarrow W^*W^* \mathcal{O}(\alpha^2\alpha_s^3)$ 14. NNLO $pp \rightarrow t\bar{t}$ 15. NNLO to VBF and $Z/\gamma+\text{jet}$	backgrounds to Higgs normalization of a benchmark process Higgs couplings and SM benchmark
Calculations including electroweak effects	
16. NNLO QCD+NLO EW for W/Z	precision calculation of a SM benchmark

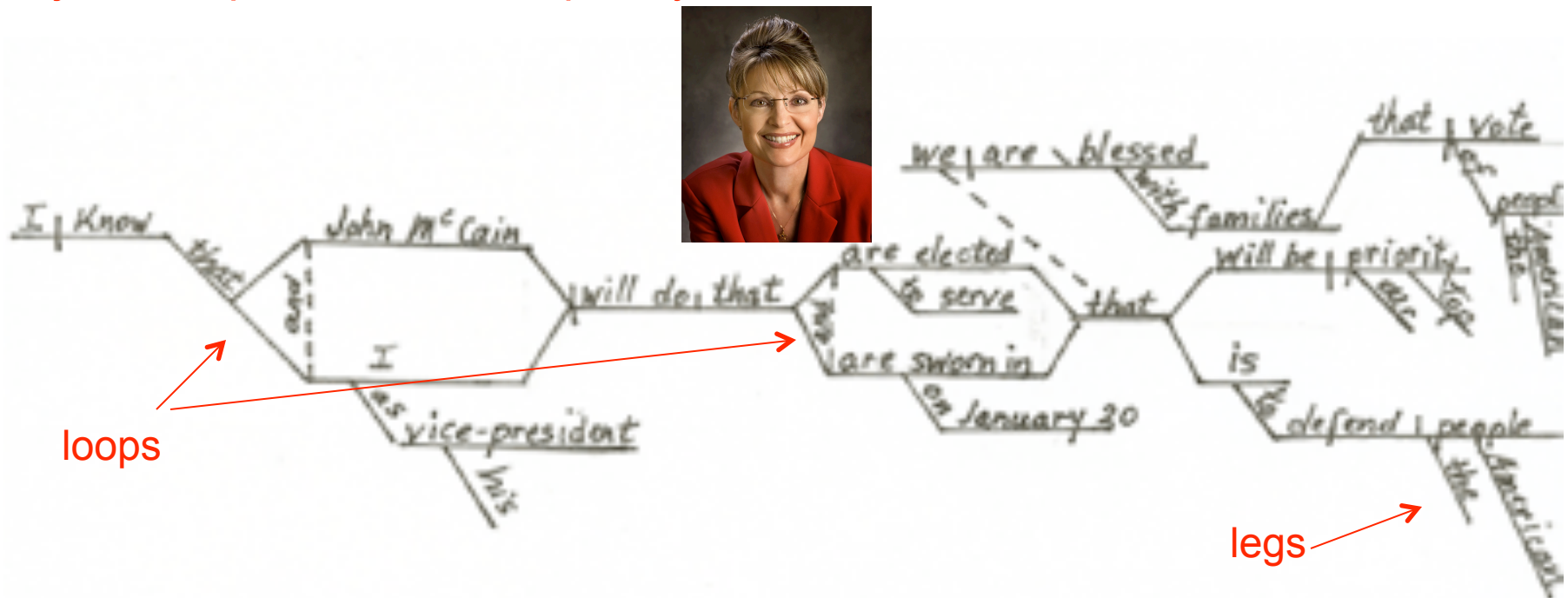
Table 1: The updated experimenter's wishlist for LHC processes

Loops and legs

2-→4 is very impressive



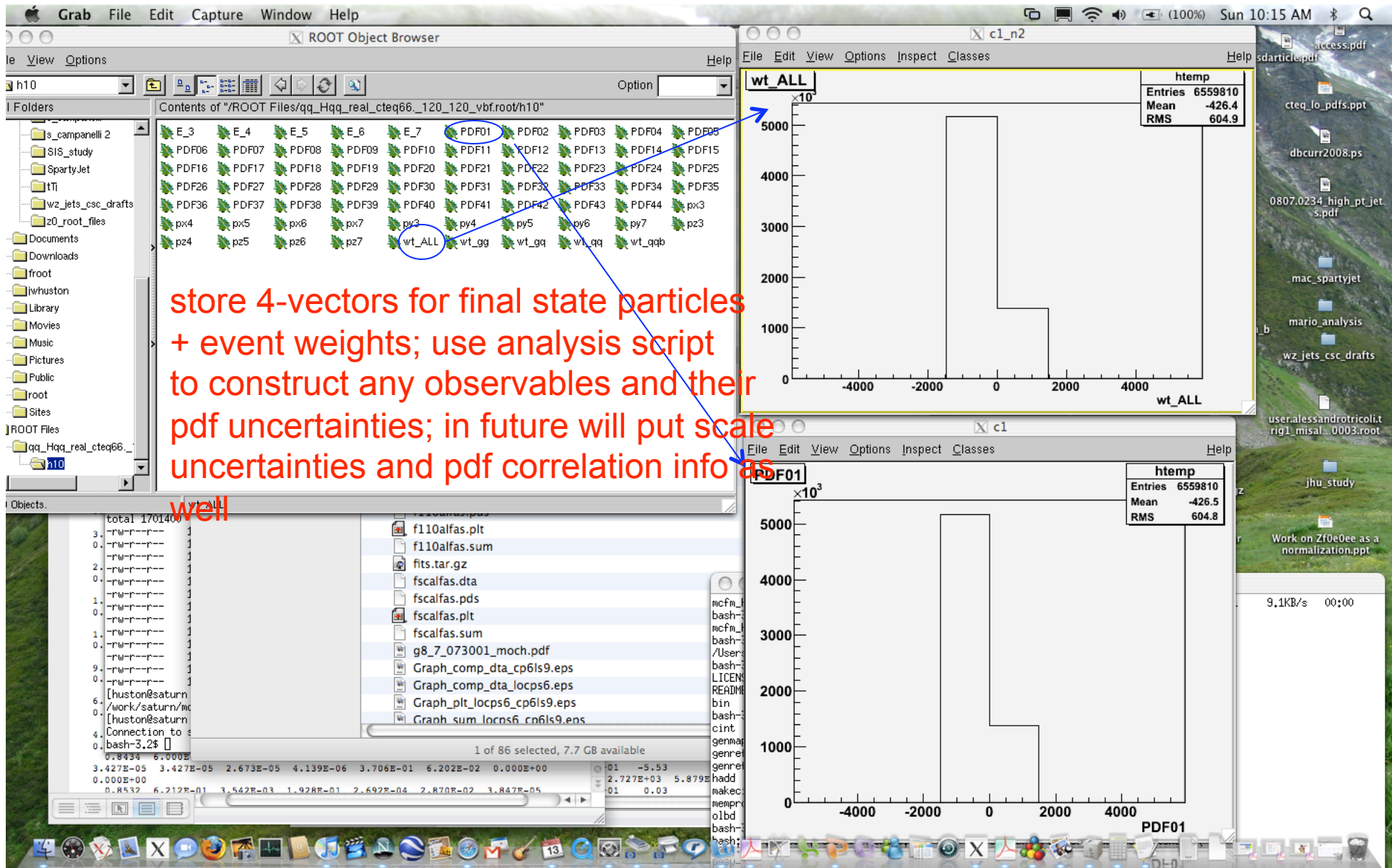
but just compare to the complexity of the sentences that Sarah Palin uses



Some issues/questions

- Once we have the calculations, how do we (experimentalists) use them?
- Best is to have NLO partonic level calculation interfaced to parton shower/hadronization
 - ◆ but that has been done only for relatively simple processes and is very (theorist) labor intensive
 - ▲ still waiting for inclusive jets in MC@NLO, for example
- Even with partonic level calculations, need public code and/or ability to write out ROOT ntuples of parton level events
 - ◆ so that can generate once with loose cuts and distributions can be re-made without the need for the lengthy re-running of the predictions
 - ◆ what is done for example with MCFM for CTEQ4LHC
 - ▲ but 10's of Gbytes for file sizes

MCFM has ROOT output built in; standard Les Houches format has been developed



Proposed common ntuple output

- A generalization of the FROOT format used in MCFM
- Writeup in NLM proceedings

Table 4: Variables stored in the proposed common ROOT ntuple output.

ROOT Tree Branch	Description
Npart/I	number of partons (incoming and outgoing)
Px[Npart]/D	Px of partons
Py[Npart]/D	Py of partons
Pz[Npart]/D	Pz of partons
E[Npart]/D	E of partons
x1/D	Bjorken-x of incoming parton 1
x2/D	Bjorken-x of incoming parton 2
id1/I	PDG particle ID of incoming parton 1
id2/I	PDF particle ID of incoming parton 2
fac_scale/D	factorization scale
ren_scale/D	renormalization scale
weight/D	global event weight
Nuwgt/I	number of user weights
user_wgts[Nuwgt]/D	user event weights
evt_no/L	unique event number (identifier)
Nptr/I	number of event pointers
evt_pointers[Nptr]/L	event pointers (identifiers of related events)
Npdfs/I	number of PDF weights
pdf_wgts[Npdfs]/D	PDF weights

```
LhaNLOEvent* evt = new LhaNLOEvent();
evt->addParticle(px1,py1,pz1,E1);
evt->setProcInfo(x1,id1,x2,id2);
evt->setRenScale(scale);
...
```

Another class `LhaNLOTreeIO` is responsible for writing the events into the ROOT tree and outputting the tree to disk. In addition to the event-wise information global data such as comments, cross sections etc can be written as well. An example is shown below:

```
LhaNLOTreeIO* writer = new LhaNLOTreeIO(); // create tree writer
writer->initWrite('test.root');
...
writer->writeComment('W+4 jets at NNLO'); // write global comments
writer->writeComment('total cross section: XYZ+/-IJK fb');
...
writer->writeEvent(*evt); // write event to tree (in event loop)
...
writer->writeTree(); // write tree to disk
```

Similarly, a tree can be read back from disk:

```
LhaNLOTreeIO* reader = new LhaNLOTreeIO(); // init reader
ierr=reader->initRead("test.root");
if (!ierr) {
    for (int i=0; i< reader->getNumberOfEvents();i++) {
        event->reset();
        ierr=reader->readEvent(i,*event);
        ...
    }
}
```


K-factors

- Often we work at LO by necessity (parton shower Monte Carlos), but would like to know the impact of NLO corrections
- K-factors (NLO/LO) can be a useful short-hand for this information
- But caveat emptor; the value of the K-factor depends on a number of things
 - ◆ PDFs used at LO and NLO
 - ◆ scale(s) at which the cross sections are evaluated
- And often the NLO corrections result in a shape change, so that one K-factor is not sufficient to modify the LO cross sections

K-factor table from CHS paper

K-factors for LHC slightly less K-factors at Tevatron K-factors with NLO PDFs at LO are more often closer to unity

Process	Typical scales		Tevatron K -factor			LHC K -factor			
	μ_0	μ_1	$\mathcal{K}(\mu_0)$	$\mathcal{K}(\mu_1)$	$\mathcal{K}'(\mu_0)$	$\mathcal{K}(\mu_0)$	$\mathcal{K}(\mu_1)$	$\mathcal{K}'(\mu_0)$	
W	m_W	$2m_W$	1.33	1.31	1.21	1.15	1.05	1.15	
$W+1\text{jet}$	m_W	p_T^{jet}	1.42	1.20	1.43	1.21	1.32	1.42	
$W+2\text{jets}$	m_W	p_T^{jet}	1.16	0.91	1.29	0.89	0.88	1.10	
$WW+\text{jet}$	m_W	$2m_W$	1.19	1.37	1.26	1.33	1.40	1.42	
$t\bar{t}$	m_t	$2m_t$	1.08	1.31	1.24	1.40	1.59	1.19	
$t\bar{t}+1\text{jet}$	m_t	$2m_t$	1.13	1.43	1.37	0.97	1.29	1.10	
$b\bar{b}$	m_b	$2m_b$	1.20	1.21	2.10	0.98	0.84	2.51	
Higgs	m_H	p_T^{jet}	2.33	–	2.33	1.72	–	2.32	
Higgs via VBF	m_H	p_T^{jet}	1.07	0.97	1.07	1.23	1.34	0.85	
Higgs+1jet	m_H	p_T^{jet}	2.02	–	2.13	1.47	–	1.90	
Higgs+2jets	m_H	p_T^{jet}	–	–	–	1.15	–	–	

Table 3: K -factors for various processes at the LHC calculated using a selection of input parameters. Have to fix this table. In all cases, the CTEQ6M PDF set is used at NLO. \mathcal{K} uses the CTEQ6L1 set at leading order, whilst \mathcal{K}' uses the same set, CTEQ6M, as at NLO and \mathcal{K}'' uses the modified LO (2-loop) PDF set. For Higgs+1,2jets, a jet cut of 40 GeV/ c and $|\eta| < 4.5$ has been applied. A cut of $p_T^{\text{jet}} > 20 \text{ GeV}/c$ has been applied for the $t\bar{t}$ +jet process, and a cut of $p_T^{\text{jet}} > 50 \text{ GeV}/c$ for WW +jet. In the W (Higgs)+2jets process the jets are separated by $\Delta R > 0.52$, whilst the VBF calculations are performed for a Higgs boson of mass 120 GeV. In each case the value of the K -factor is compared at two often-used scale choices, where the scale indicated is used for both renormalization and factorization scales.

Shapes of distributions may be different at NLO than at LO, but sometimes it is still useful to define a K -factor.

Note the value of the K -factor depends critically on its definition.

Go back to K-factor table

- Some rules-of-thumb
- NLO corrections are larger for processes in which there is a great deal of color annihilation
 - ◆ $gg \rightarrow \text{Higgs}$
 - ◆ $gg \rightarrow \gamma\gamma$
 - ◆ $K(gg \rightarrow tT) > K(qQ \rightarrow tT)$
 - ◆ these gg initial states want to radiate like crazy (see Sudakovs)
- NLO corrections decrease as more final-state legs are added
 - ◆ $K(gg \rightarrow \text{Higgs} + 2 \text{ jets}) < K(gg \rightarrow \text{Higgs} + 1 \text{ jet}) < K(gg \rightarrow \text{Higgs})$
 - ◆ unless can access new initial state gluon channel
- Can we generalize for uncalculated HO processes?
- What about effect of jet vetoes on K-factors? Signal processes compared to background. Of current interest.

Process	Typical scales		Tevatron K -factor			LHC K -factor		
	μ_0	μ_1	$\mathcal{K}(\mu_0)$	$\mathcal{K}(\mu_1)$	$\mathcal{K}'(\mu_0)$	$\mathcal{K}(\mu_0)$	$\mathcal{K}(\mu_1)$	$\mathcal{K}'(\mu_0)$
W	m_W	$2m_W$	1.33	1.31	1.21	1.15	1.05	1.15
$W+1\text{jet}$	m_W	p_T^{jet}	1.42	1.20	1.43	1.21	1.32	1.42
$W+2\text{jets}$	m_W	p_T^{jet}	1.16	0.91	1.29	0.89	0.88	1.10
$WW+\text{jet}$	m_W	$2m_W$	1.19	1.37	1.26	1.33	1.40	1.42
$t\bar{t}$	m_t	$2m_t$	1.08	1.31	1.24	1.40	1.59	1.48
$t\bar{t}+1\text{jet}$	m_t	$2m_t$	1.13	1.43	1.37	0.97	1.29	1.10
$b\bar{b}$	m_b	$2m_b$	1.20	1.21	2.10	0.98	0.84	2.51
Higgs	m_H	p_T^{jet}	2.33	—	2.33	1.72	—	2.32
Higgs via VBF	m_H	p_T^{jet}	1.07	0.97	1.07	1.23	1.34	1.09
Higgs+1jet	m_H	p_T^{jet}	2.02	—	2.13	1.47	—	1.90
Higgs+2jets	m_H	p_T^{jet}	—	—	—	1.15	—	—

Table 2: K -factors for various processes at the Tevatron and the LHC calculated using a selection of input parameters. In all cases, the CTEQ6M PDF set is used at NLO. \mathcal{K} uses the CTEQ6L1 set at leading order, whilst \mathcal{K}' uses the same set, CTEQ6M, as at NLO. For most of the processes listed, jets satisfy the requirements $p_T > 15 \text{ GeV}/c$ and $|\eta| < 2.5$ (5.0) at the Tevatron (LHC). For Higgs+1,2jets, a jet cut of $40 \text{ GeV}/c$ and $|\eta| < 4.5$ has been applied. A cut of $p_T^{\text{jet}} > 20 \text{ GeV}/c$ has been applied for the $t\bar{t}$ -jet process, and a cut of $p_T^{\text{jet}} > 50 \text{ GeV}/c$ for WW +jet. In the $W(\text{Higgs})+2\text{jets}$ process the jets are separated by $\Delta R > 0.52$, whilst the VBF calculations are performed for a Higgs boson of mass 120 GeV . In each case the value of the K -factor is compared at two often-used scale choices, where the scale indicated is used for both renormalization and factorization scales.

Casimir for biggest color representation final state can be in

Simplistic rule

$$C_{i1} + C_{i2} - C_{f,\text{max}}$$

L. Dixon

Casimir color factors for initial state

Shape dependence of a K-factor

- Inclusive jet production probes very wide x, Q^2 range along with varying mixture of gg, gq , and qq subprocesses
- PDF uncertainties are significant at high p_T
- Over limited range of p_T and y , can approximate effect of NLO corrections by K-factor but not in general
 - ◆ in particular note that for forward rapidities, K-factor $\ll 1$
 - ◆ LO predictions will be large overestimates
 - ◆ this is true for both the Tevatron and for the LHC

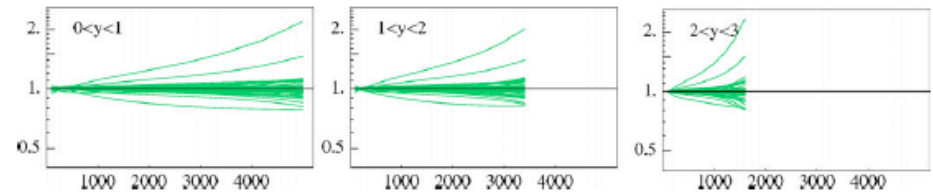


Figure 105. The ratios of the jet cross section predictions for the LHC using the CTEQ6.1 error pdfs to the prediction using the central pdf. The extremes are produced by eigenvector 15.

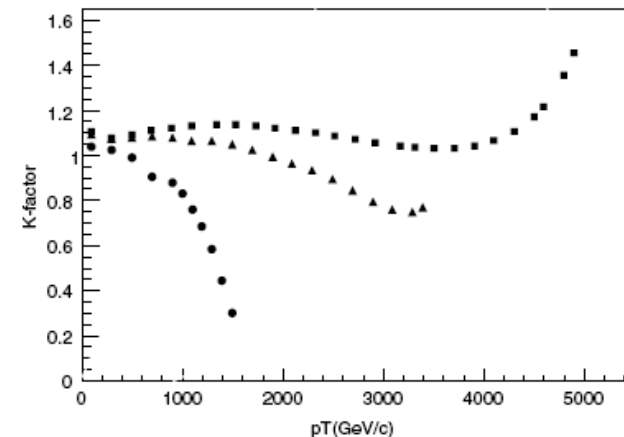


Figure 106. The ratios of the NLO to LO jet cross section predictions for the LHC using the CTEQ6.1 pdfs for the three different rapidity regions (0-1 (squares), 1-2 (triangles), 2-3 (circles)).

Aside: Why K-factors < 1 for inclusive jet production?

- Write cross section indicating explicit scale-dependent terms
- First term (lowest order) in Eq. 3 leads to monotonically decreasing behavior as scale increases (the LO piece)
- Second term is negative for $\mu < p_T$, positive for $\mu > p_T$
- Third term is negative for factorization scale $M < p_T$
- Fourth term has same dependence as lowest order term
- Thus, lines one and four give contributions which decrease monotonically with increasing scale while lines two and three start out negative, reach zero when the scales are equal to p_T , and are positive for larger scales
- At NLO, result is a roughly parabolic behavior

Consider a large transverse momentum process such as the single jet inclusive cross section involving only massless partons. Furthermore, in order to simplify the notation, suppose that the transverse momentum is sufficiently large that only the quark distributions need be considered. In the following, a sum over quark flavors is implied. Schematically, one can write the lowest order cross section as

$$E \frac{d^3\sigma}{dp^3} \equiv \sigma = a^2(\mu) \hat{\sigma}_B \otimes q(M) \otimes q(M) \quad (1)$$

where $a(\mu) = \alpha_s(\mu)/2\pi$ and the lowest order parton-parton scattering cross section is denoted by $\hat{\sigma}_B$. The renormalization and factorization scales are denoted by μ and M , respectively. In addition, various overall factors have been absorbed into the definition of $\hat{\sigma}_B$. The symbol \otimes denotes a convolution defined as

$$f \otimes g = \int_x^1 \frac{dy}{y} f\left(\frac{x}{y}\right) g(y). \quad (2)$$

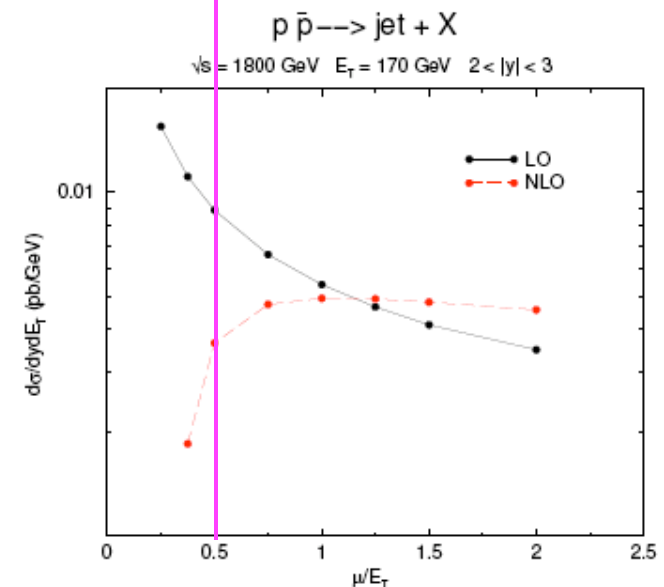
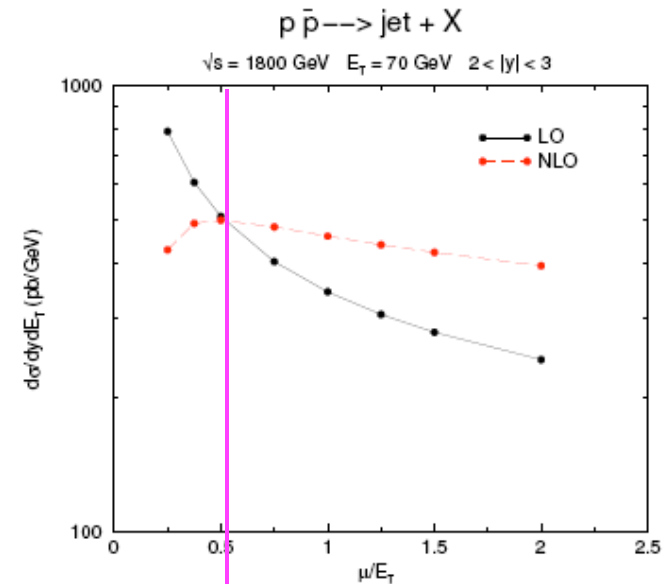
When one calculates the $\mathcal{O}(\alpha_s^3)$ contributions to the inclusive cross section, the result can be written as

$$\begin{aligned} (1) \quad \sigma &= a^2(\mu) \hat{\sigma}_B \otimes q(M) \otimes q(M) \\ (2) \quad &+ 2a^3(\mu) b \ln(\mu/p_T) \hat{\sigma}_B \otimes q(M) \otimes q(M) \\ (3) \quad &+ 2a^3(\mu) \ln(p_T/M) P_{qq} \otimes \hat{\sigma}_B \otimes q(M) \otimes q(M) \\ (4) \quad &+ a^3(\mu) K \otimes q(M) \otimes q(M). \end{aligned} \quad (3)$$

In writing Eq. (3), specific logarithms associated with the running coupling and the scale dependence of the parton distributions have been explicitly displayed; the remaining higher order corrections have been collected in the function K in the last line of Eq. (3). The μ

Why K-factor for inclusive jets < 1?

- First term (lowest order) in (3) leads to monotonically decreasing behavior as scale increases
- Second term is negative for $\mu < p_T$, positive for $\mu > p_T$
- Third term is negative for factorization scale $M < p_T$
- Fourth term has same dependence as lowest order term
- Thus, lines one and four give contributions which decrease monotonically with increasing scale while lines two and three start out negative, reach zero when the scales are equal to p_T , and are positive for larger scales
- NLO parabola moves out towards higher scales for forward region
- Scale of $E_T/2$ results in a K-factor of ~ 1 for low E_T , < 1 for high E_T for forward rapidities at Tevatron, and at the LHC



Consider the $W + 3$ jets process

Process ($V \in \{Z, W, \gamma\}$)	Comments
Calculations completed since Les Houches 2005	
1. $pp \rightarrow VV\text{jet}$	$WW\text{jet}$ completed by Dittmaier/Kallweit/Uwer [4, 5]; Campbell/Ellis/Zanderighi [6]. $ZZ\text{jet}$ completed by Binoth/Gleisberg/Karg/Kauer/Sanguinetti [7] NLO QCD to the gg channel completed by Campbell/Ellis/Zanderighi [8]; NLO QCD+EW to the VBF channel completed by Ciccolini/Denner/Dittmaier [9, 10] ZZZ completed by Lazopoulos/Melnikov/Petriello [11] and WWZ by Hankele/Zeppenfeld [12] (see also Binoth/Ossola/Papadopoulos/Pittau [13])
2. $pp \rightarrow \text{Higgs}+2\text{jets}$	
3. $pp \rightarrow V V V$	
4. $pp \rightarrow t\bar{t} b\bar{b}$	
5. $pp \rightarrow V+3\text{jets}$	relevant for $t\bar{t}H$ computed by Bredenstein/Denner/Dittmaier/Pozzorini [14, 15] and Bevilacqua/Czakon/Papadopoulos/Pittau/Worek [16] calculated by the Blackhat/Sherpa [17] and Rocket [18] collaborations
Calculations remaining from Les Houches 2005	
6. $pp \rightarrow t\bar{t}+2\text{jets}$	relevant for $t\bar{t}H$ computed by Bevilacqua/Czakon/Papadopoulos/Worek [19] relevant for $VBF \rightarrow H \rightarrow VV, t\bar{t}H$ relevant for $VBF \rightarrow H \rightarrow VV$ VBF contributions calculated by (Bozzi/Jäger/Oleari/Zeppenfeld [20–22])
7. $pp \rightarrow VV b\bar{b}$,	
8. $pp \rightarrow VV+2\text{jets}$	
NLO calculations added to list in 2007	
9. $pp \rightarrow b\bar{b}b\bar{b}$	$q\bar{q}$ channel calculated by Golem collaboration [23]
NLO calculations added to list in 2009	
10. $pp \rightarrow V+4\text{ jets}$ 11. $pp \rightarrow Wb\bar{b}j$ 12. $pp \rightarrow t\bar{t}t\bar{t}$	top pair production, various new physics signatures top, new physics signatures various new physics signatures
Calculations beyond NLO added in 2007	
13. $gg \rightarrow W^*W^* \mathcal{O}(\alpha^2\alpha_s^3)$ 14. NNLO $pp \rightarrow t\bar{t}$ 15. NNLO to VBF and $Z/\gamma+\text{jet}$	backgrounds to Higgs normalization of a benchmark process Higgs couplings and SM benchmark
Calculations including electroweak effects	
16. NNLO QCD+NLO EW for W/Z	precision calculation of a SM benchmark

Table 1: The updated experimenter's wishlist for LHC processes

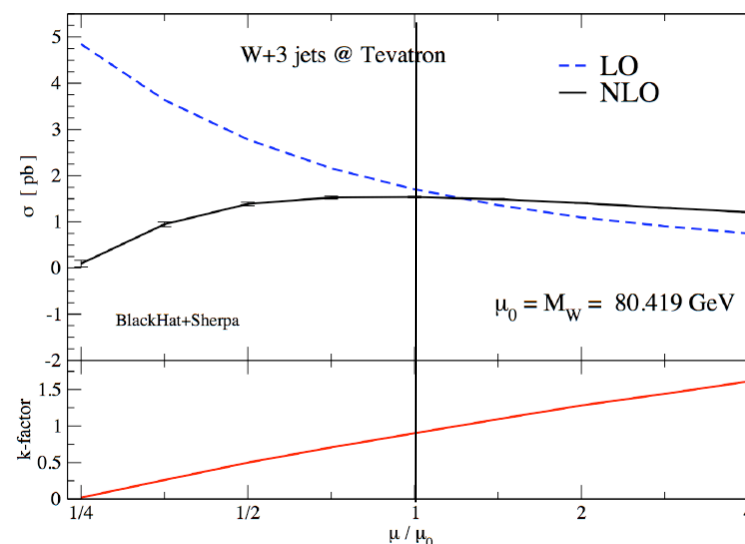
Now consider W + 3 jets

Consider a scale of m_W for W + 1,2,3 jets. We see the K-factors for W + 1,2 jets in the table below, and recently the NLO corrections for W + 3 jets have been calculated, allowing us to estimate the K-factors for that process.

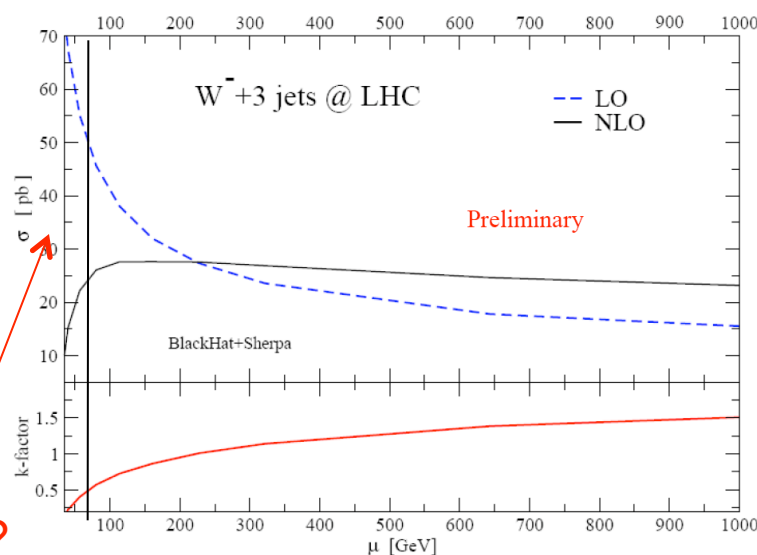
Process	Typical scales		Tevatron K -factor			LHC K -factor			
	μ_0	μ_1	$\mathcal{K}(\mu_0)$	$\mathcal{K}(\mu_1)$	$\mathcal{K}'(\mu_0)$	$\mathcal{K}(\mu_0)$	$\mathcal{K}(\mu_1)$	$\mathcal{K}'(\mu_0)$	$\mathcal{K}''(\mu_0)$
W	m_W	$2m_W$	1.33	1.31	1.21	1.15	1.05	1.15	0.95
W+1jet	m_W	p_T^{jet}	1.42	1.20	1.43	1.21	1.32	1.42	0.99
W+2jets	m_W	p_T^{jet}	1.16	0.91	1.29	0.89	0.88	1.10	0.90
WW+jet	m_W	$2m_W$	1.19	1.37	1.26	1.33	1.40	1.42	1.10
$t\bar{t}$	m_t	$2m_t$	1.08	1.31	1.24	1.40	1.59	1.19	1.09
$t\bar{t}$ +1jet	m_t	$2m_t$	1.13	1.43	1.37	0.97	1.29	1.10	0.85
$b\bar{b}$	m_b	$2m_b$	1.20	1.21	2.10	0.98	0.84	2.51	—
Higgs	m_H	p_T^{jet}	2.33	—	2.33	1.72	—	2.32	1.43
Higgs via VBF	m_H	p_T^{jet}	1.07	0.97	1.07	1.23	1.34	0.85	0.78
Higgs+1jet	m_H	p_T^{jet}	2.02	—	2.13	1.47	—	1.90	1.33
Higgs+2jets	m_H	p_T^{jet}	—	—	—	1.15	—	—	1.13

Table 3: K -factors for various processes at the LHC calculated using a selection of input parameters. Have to fix this table. In all cases, the CTEQ6M PDF set is used at NLO. \mathcal{K} uses the CTEQ6L1 set at leading order, whilst \mathcal{K}' uses the same set, CTEQ6M, as at NLO and \mathcal{K}'' uses the modified LO (2-loop) PDF set. For Higgs+1,2jets, a jet cut of 40 GeV/c and $|\eta| < 4.5$ has been applied. A cut of $p_T^{\text{jet}} > 20$ GeV/c has been applied for the $t\bar{t}$ -jet process, and a cut of $p_T^{\text{jet}} > 50$ GeV/c for WW +jet. In the W(Higgs)+2jets process the jets are separated by $\Delta R > 0.52$, whilst the VBF calculations are performed for a Higgs boson of mass 120 GeV. In each case the value of the K -factor is compared at two often-used scale choices, where the scale indicated is used for both renormalization and factorization scales.

Is the K-factor (at m_W) at the LHC surprising?



LHC total cross section



Is the K-factor (at m_W) at the LHC surprising?

The K-factors for W + jets ($p_T > 30$ GeV/c) fall near a straight line, as do the K-factors for the Tevatron. By definition, the K-factors for Higgs + jets fall on a straight line.

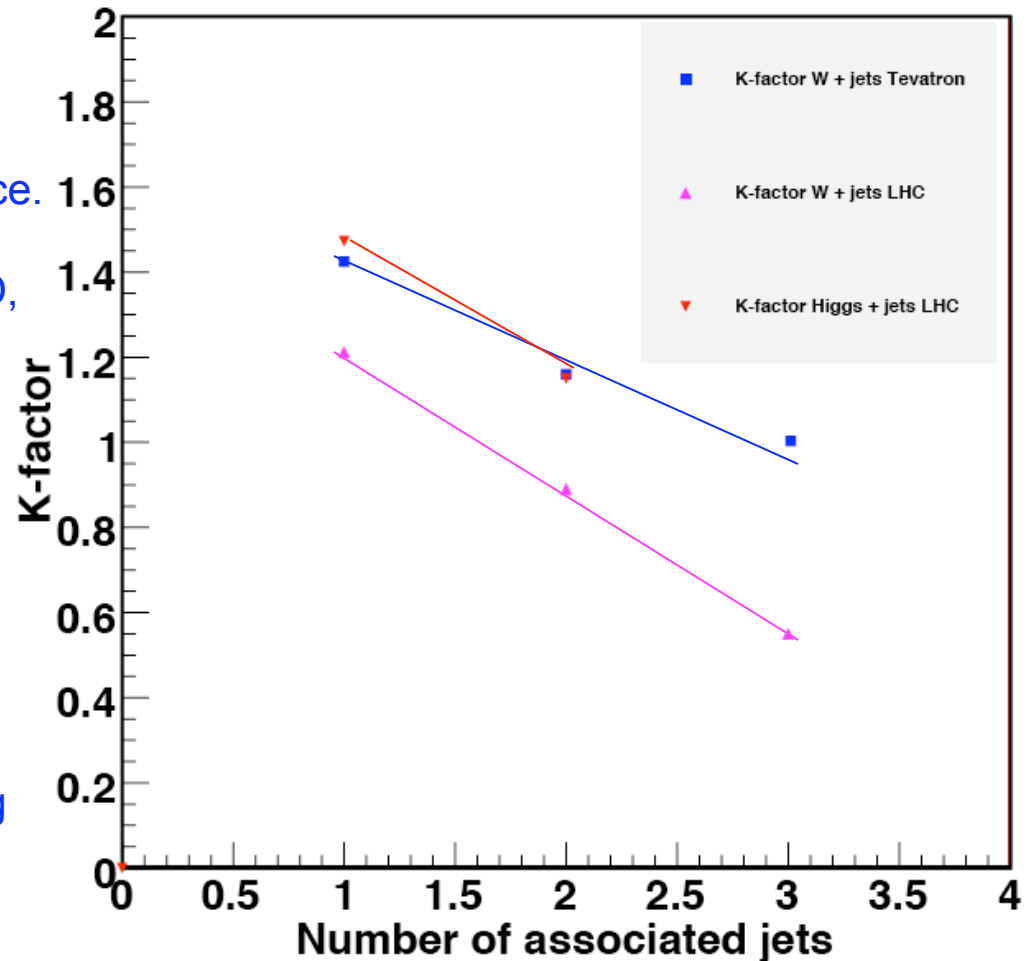
Nothing special about m_W ; just a typical choice.

The only way to know a cross section to NLO, say for W + 4 jets or Higgs + 3 jets, is to calculate it, but in lieu of the calculations, especially for observables that we have deemed important at Les Houches, can we make some rules of thumb?

Related to this is:

- understanding the reduced scale dependences/pdf uncertainties for cross section ratios we have been discussing
- scale choices at LO for cross sections uncalculated at NLO

K-factors at scale m_W/m_H as fn of # of associated jets



Is the K-factor (at m_W) at the LHC surprising?

The K-factors for W + jets ($p_T > 30$ GeV/c) fall near a straight line, as do the K-factors for the Tevatron. By definition, the K-factors for Higgs + jets fall on a straight line.

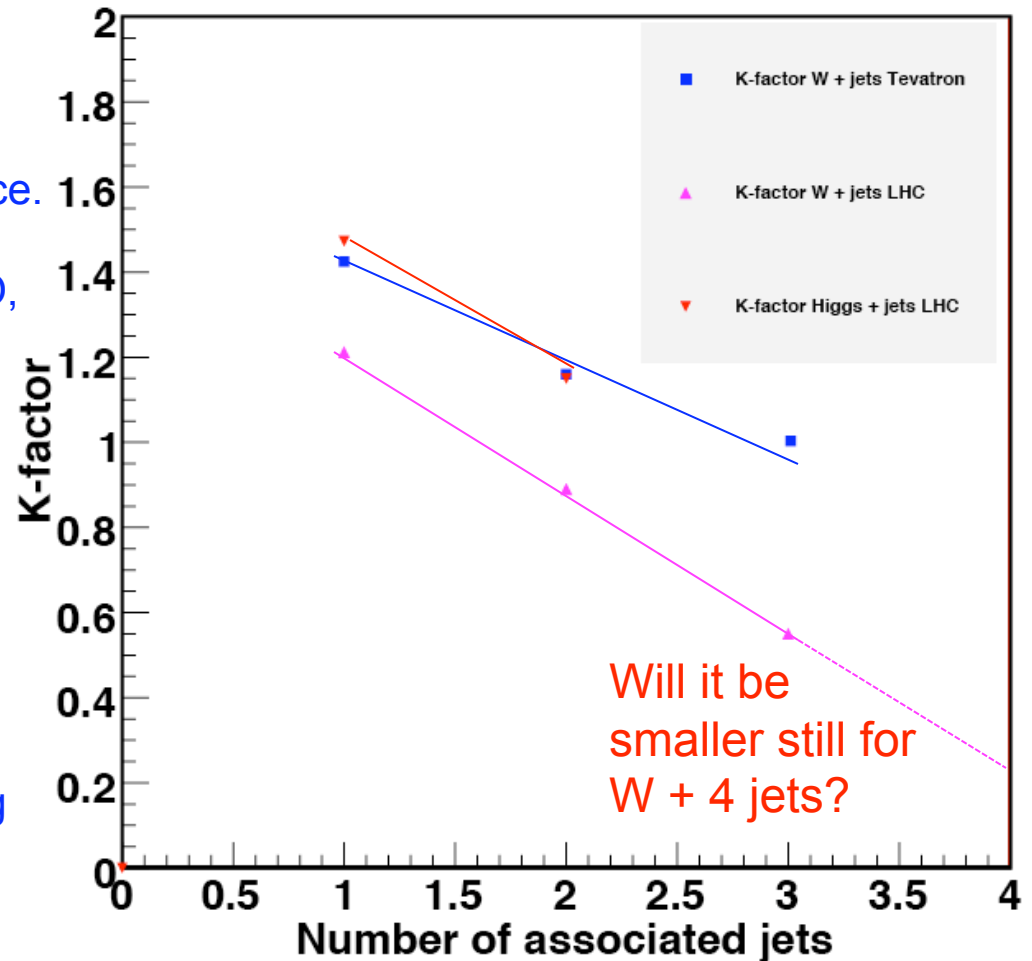
Nothing special about m_W ; just a typical choice.

The only way to know a cross section to NLO, say for W + 4 jets or Higgs + 3 jets, is to calculate it, but in lieu of the calculations, especially for observables that we have deemed important at Les Houches, can we make rules of thumb?

Related to this is:

- understanding the reduced scale dependences/pdf uncertainties for the cross section ratios we have been discussing
- scale choices at LO for cross sections calculated at NLO
- scale choices at LO for cross sections uncalculated at NLO

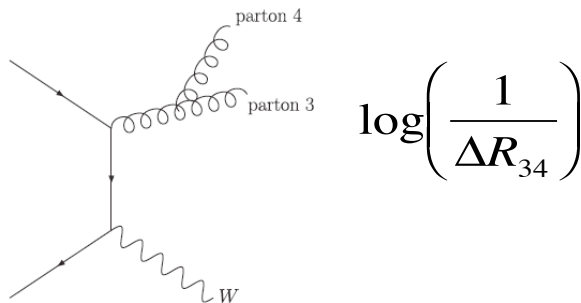
K-factors at scale m_W/m_H as fn of # of associated jets



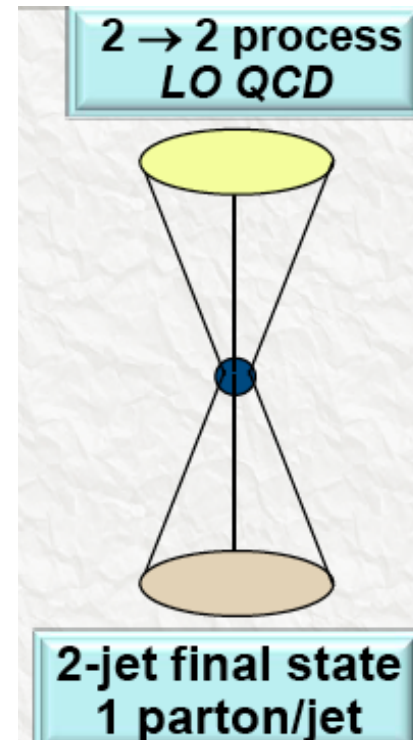
To understand this further, we have to discuss jet algorithms

Jet algorithms at LO

- At (fixed) LO, 1 parton = 1 jet
 - ◆ why not more than 1? I have to put a ΔR cut on the separation between two partons; otherwise, there's a collinear divergence. LO parton shower programs effectively put in such a cutoff
 - ◆ Remember the collinear singularity



- But at NLO, I have to deal with more than 1 parton in a jet, and so now I have to talk about how to cluster those partons
 - ◆ i.e. jet algorithms



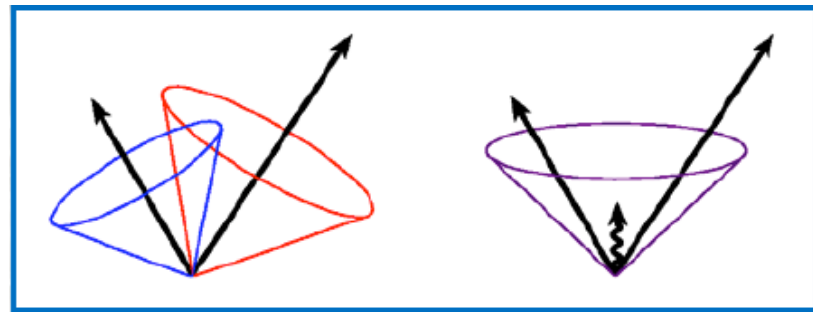
Jet algorithms at NLO

- At NLO, there can be two partons in a jet, life becomes more interesting and we have to start talking about jet algorithms to define jets
 - ◆ the addition of the real and virtual terms at NLO cancels the divergence.
- A jet algorithm is based on some measure of localization of the expected collinear spray of particles
- Start with an inclusive list of particles/partons/calorimeter towers/topoclusters
- End with lists of same for each jet
- ...and a list of particles... not in any jet; for example, remnants of the initial hadrons
- Two broad classes of jet algorithms
 - ◆ cluster according to proximity in space: cone algorithms
 - ◆ cluster according to proximity in momenta: k_T algorithms

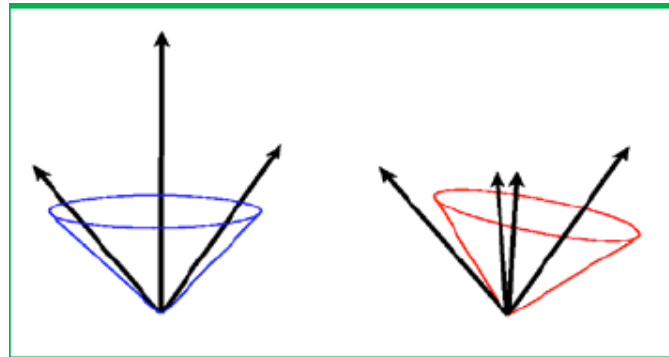
What do I want out of a jet algorithm?

- It should be fully specified, including defining in detail any pre-clustering, merging and splitting issues
- It should be simple to implement in an experimental analysis, and should be independent of the structure of the detector
- It should be boost-invariant
- It should be simple to implement in a theoretical calculation
 - ◆ it should be defined at any order in perturbation theory
 - ◆ it should yield a finite cross section at any order in perturbation theory
 - ◆ it should yield a cross section that is relatively insensitive to hadronization effects

- It should be IR safe, i.e. adding a soft gluon should not change the results of the jet clustering

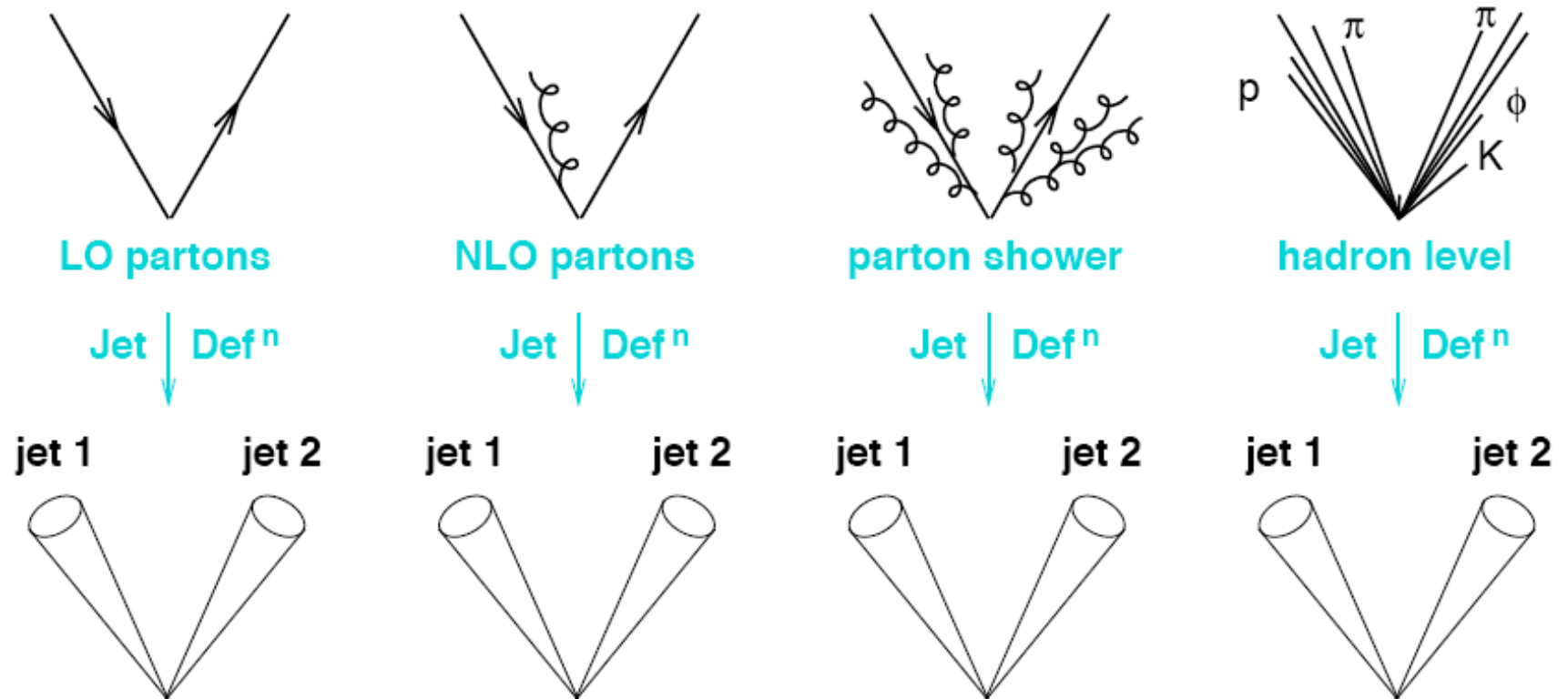


- It should be collinear safe, i.e. splitting one parton into two collinear partons should not change the results of the jet clustering



Jet algorithms

- The algorithm should behave in a similar manner (as much as possible) at the parton, particle and detector levels. Note that differences between levels can unavoidably creep in.



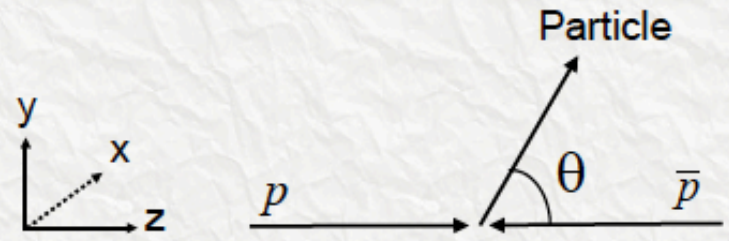
Projection to jets should be resilient to QCD effects

Some kinematic definitions

Rapidity (y) and Pseudo-rapidity (η)

$$y \equiv \frac{1}{2} \ln \frac{E + p_z}{E - p_z} = \frac{1}{2} \ln \frac{1 + \beta \cos \theta}{1 - \beta \cos \theta}$$

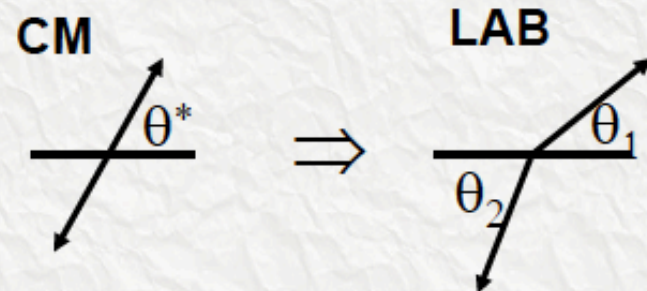
$$\beta \cos \theta = \tanh y \quad \text{where } \beta = p/E$$



In the limit $\beta \rightarrow 1$ (or $m \ll p_T$) then

$$\eta \equiv y|_{m=0} = \frac{1}{2} \ln \frac{1 + \cos \theta}{1 - \cos \theta} = -\ln \tan \frac{\theta}{2}$$

**LAB System \neq parton-parton
CM system**



$\Delta\eta$ and p_T are invariant under longitudinal boosts

Some kinematic definitions

To satisfy listed requirements for jet algorithms, use p_T, y and ϕ to characterize jets

Transverse Energy/Momentum

$$E_T^2 \equiv p_x^2 + p_y^2 + m^2 = p_T^2 + m^2 = E^2 - p_z^2$$

Invariant Mass

$$\begin{aligned} M_{12}^2 &\equiv (p_1^\mu + p_2^\mu)(p_{1\mu} + p_{2\mu}) \\ &= m_1^2 + m_2^2 + 2(E_1 E_2 - \mathbf{p}_1 \cdot \mathbf{p}_2) \\ &\xrightarrow{m_1, m_2 \rightarrow 0} 2E_{T1} E_{T2} (\cosh \Delta\eta - \cos \Delta\phi) \end{aligned}$$

Partonic Momentum Fractions

$$\begin{aligned} x_1 &= (e^{\eta_1} + e^{\eta_2}) E_T / \sqrt{s} \\ x_2 &= (e^{-\eta_1} + e^{-\eta_2}) E_T / \sqrt{s} \end{aligned}$$

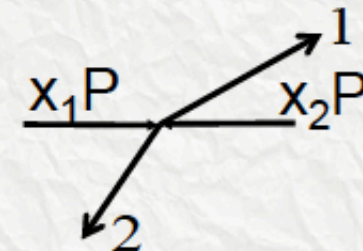
$$\text{Parton CM (energy)}^2 \rightarrow \hat{s} = x_a x_b s$$

$$p_z = E \tanh y$$

$$E = E_T \cosh y$$

$$p_z = E_T \sinh y$$

$$p_T \equiv p \sin \theta \xrightarrow{m \rightarrow 0} E_T$$



$$x_T \equiv 2E_T / \sqrt{s} = x_{1,2} (\eta_{1,2} = 0)$$

$$0 < x_1, x_2 < 1$$

$$x_T^2 < x_1 x_2 < 1$$

(Legacy) cone algorithms

- The cone algorithm is most often used in hadron-hadron colliders

- ◆ perhaps most intuitive
- ◆ draw a cone of radius R in η - ϕ space

$$R_{\text{cone}} = \sqrt{(\Delta\eta)^2 + (\Delta\phi)^2}$$

- But where to start the cone?

- ◆ use 'seeds' (towers, particles, partons...) of energy ~ 1 GeV to save computing time

streetlight approach

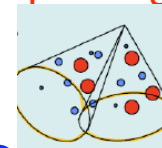


- ◆ combine seed towers with other towers within a radius R of the seed tower
- ◆ re-calculate jet centroid using new list of towers... inside cone
- ◆ lather, rinse, iterate until a stable solution is found

typically use $R \sim 0.7$ for inclusive measurements; $R \sim 0.4$ for *complex* measurements, such as t-tbar

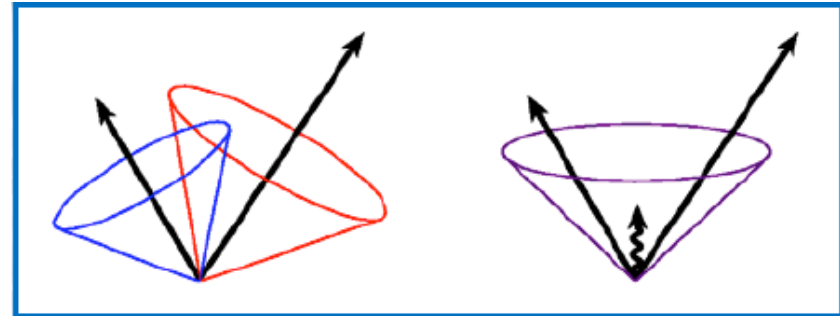


- But you may end up with overlapping jet cones (starting from different jet seeds)
- So need to come up with a provision for splitting/merging
 - ◆ merge 2 jets if overlap energy is $> f \cdot p_T$ (smaller jet)
 - ◆ $f = 0.50 - 0.75$
- Note: partons (at NLO) don't know nothing about splitting/merging
 - ◆ experience says $f = 0.75$ is best



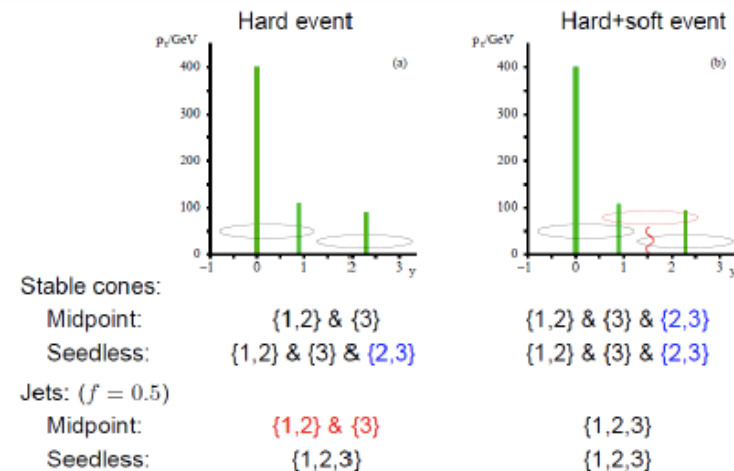
Midpoint cone algorithm

- But this type of cone algorithm is not infra-red safe, since the two partons in the figure on the right will/will not be clustered into a single jet depending on whether or not a soft gluon is present at the midpoint
 - ◆ also (in Run 1 at the Tevatron) used E_T and η , rather than p_T and y
- Fundamental difference between data and fixed order pert QCD
 - ◆ data has “seeds” everywhere
- So the Midpoint algorithm was devised
 - ◆ seeds were placed at the midpoints between nearby protojets
 - ◆ used in Run 2 at the Tevatron



- this works for 2->3 final states (NLO inclusive), but not for 2->4 (NNLO inclusive) where I may cluster 3 partons in 1 jet

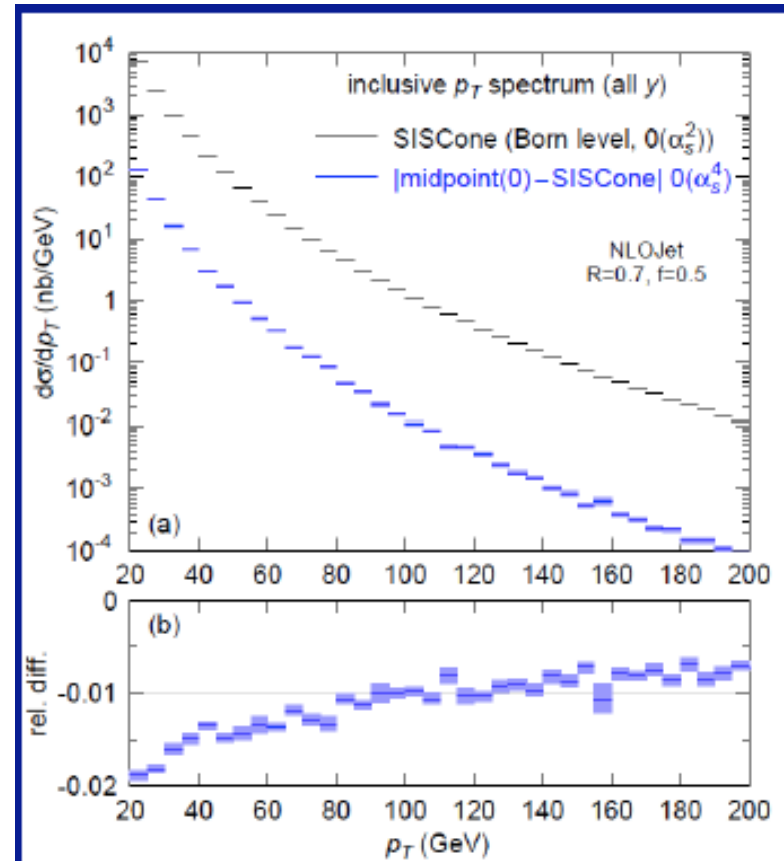
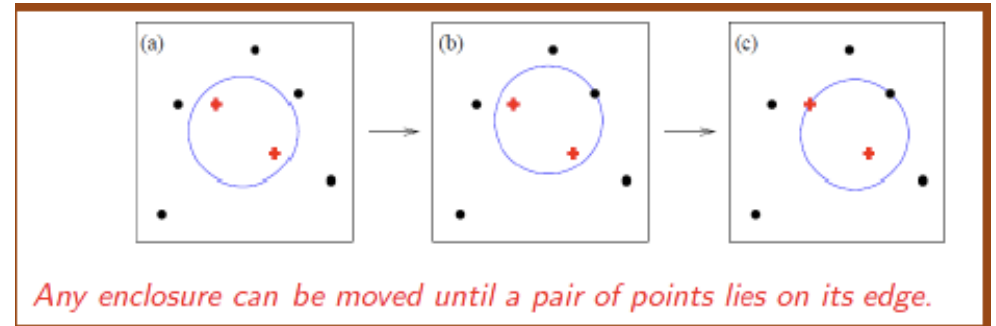
Midpoint IR Unsafety



→ IR unsafety of the midpoint algorithm

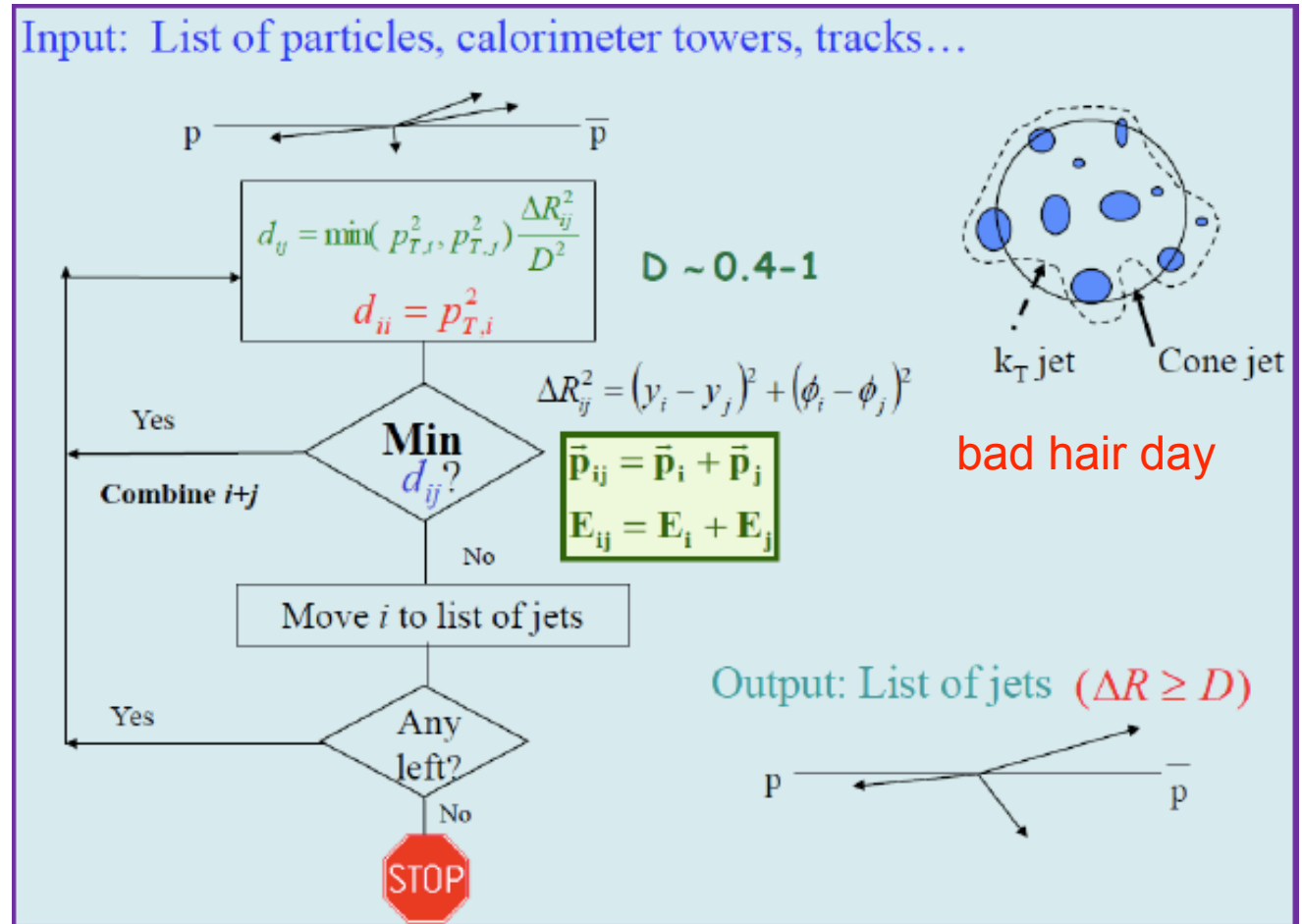
Seedless cone algorithm

- Put seeds everywhere
- Can be time-consuming
- Enter the SISCone algorithm
 - ◆ Seedless Infrared Safe Cone jet algorithm
 - ◆ G. Salam, G. Soyez, arXiv: 0704.0292
- ...uses a geometric approach to find all distinct cones
- ...with a speed similar to that of the Midpoint algorithm
- Still have the split/merge issue
- ...and the issue of *dark towers*
- Differences with the midpoint algorithm typically of the order of 1 percent or so in practice
 - ◆ see later discussion, however



k_T (recombination) algorithms

- Cluster particles nearby in momentum space first
- The k_T algorithm is IR and collinear safe
- No overlapping of jets
- No biases from seed towers
- But the jets are sensitive to soft particles and the area can depend on pileup



The k_T family of jet algorithms

- $p=1$

- ◆ the regular k_T jet algorithm

$$d_{ij} = \min(p_{T,i}^{2p}, p_{T,j}^{2p}) \frac{\Delta R_{ij}^2}{D^2}$$

- $p=0$

- ◆ Cambridge-Aachen algorithm

$$d_{ii} = p_{T,i}^{2p}$$

- $p=-1$

- ◆ anti- k_T jet algorithm
- ◆ Cacciari, Salam, Soyez '08
- ◆ also P-A Delsart '07
- ◆ soft particles will first cluster with hard particles before clustering among themselves
- ◆ no split/merge
- ◆ leads mostly to constant area hard jets

→ • #1 algorithm for ATLAS, CMS

Jet algorithms at LO/NLO

- Remember at LO, 1 parton = 1 jet
- By choosing a jet algorithm with size parameter D , we are requiring any two partons to be $> D$ apart
- The matrix elements have $1/\Delta R$ poles, so larger D means smaller cross sections
 - it's because of the poles that we have to make a ΔR cut
- At NLO, there can be two (or more) partons in a jet and jets for the first time can have some structure
 - we don't need a ΔR cut, since the virtual corrections cancel the collinear singularity from the gluon emission
 - but there are residual logs that can become important if D is too small
- Increasing the size parameter D increases the phase space for including an extra gluon in the jet, and thus increases the cross section at NLO (in most cases)

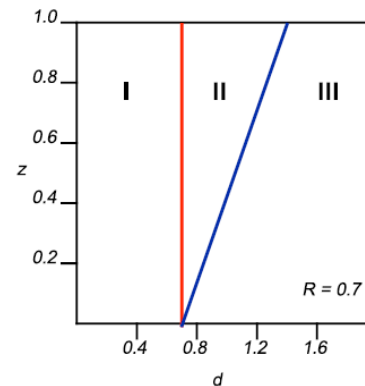
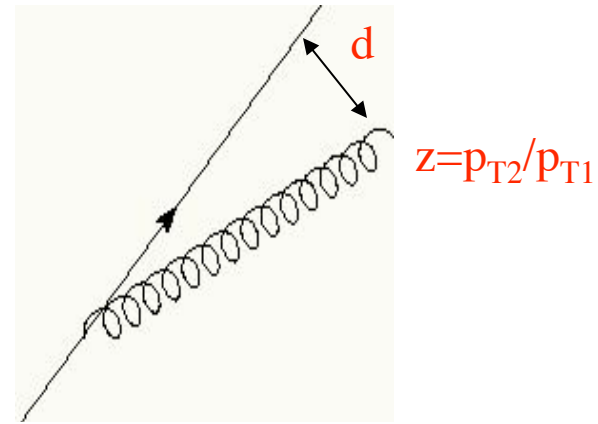


Figure 22. The parameter space (d, Z) for which two partons will be merged into a single jet.

For $D=R_{\text{cone}}$,
 Region I = k_T
 jets, Region II
 (nominally) =
 cone jets; I say
 nominally
 because in data
 not all of Region
 II is included for
 cone jets

→ not true for WbB, for example

Jets at NLO continued

- Construct what is called a Snowmass potential

shown in Figure 50, where the towers unclustered into any jet are shaded black. A simple way of understanding these dark towers begins by defining a “Snowmass potential” in terms of the 2-dimensional vector $\vec{r} = (y, \phi)$ via

$$V(\vec{r}) = -\frac{1}{2} \sum_j p_{T,j} \left(R_{cone}^2 - (\vec{r}_j - \vec{r})^2 \right) \Theta \left(R_{cone}^2 - (\vec{r}_j - \vec{r})^2 \right). \quad (39)$$

The flow is then driven by the “force” $\vec{F}(\vec{r}) = -\vec{\nabla} V(\vec{r})$ which is thus given by,

$$\begin{aligned} \vec{F}(\vec{r}) &= \sum_j p_{T,j} (\vec{r}_j - \vec{r}) \Theta \left(R_{cone}^2 - (\vec{r}_j - \vec{r})^2 \right) \\ &= \left(\vec{r}_{C(\vec{r})} - \vec{r} \right) \sum_{j \in C(\vec{r})} p_{T,j}, \end{aligned} \quad (40)$$

where $\vec{r}_{C(\vec{r})} = (\bar{y}_{C(\vec{r})}, \bar{\phi}_{C(\vec{r})})$ and the sum runs over $j \in C(\vec{r})$ such that $\sqrt{(y_j - y)^2 + (\phi_j - \phi)^2} \leq R_{cone}$. As desired, this force pushes the cone to the stable cone position.

- The minima of the potential function indicates the positions of the stable cone solutions
 - the derivative of the potential function is the force that shows the direction of flow of the iterated cone
- The midpoint solution contains both partons

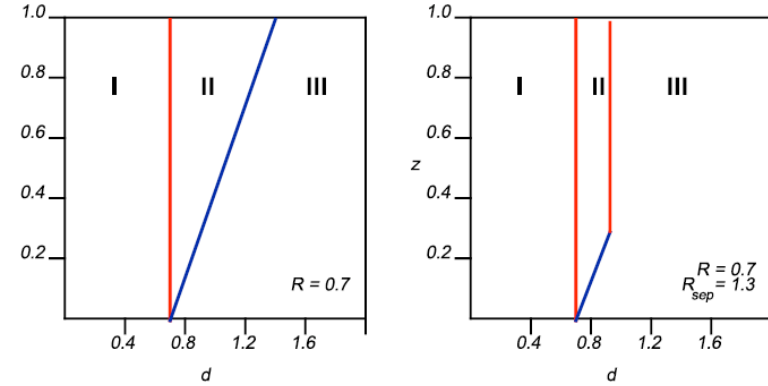


Figure 22. The parameter space (d, Z) for which two partons will be merged into a single jet.

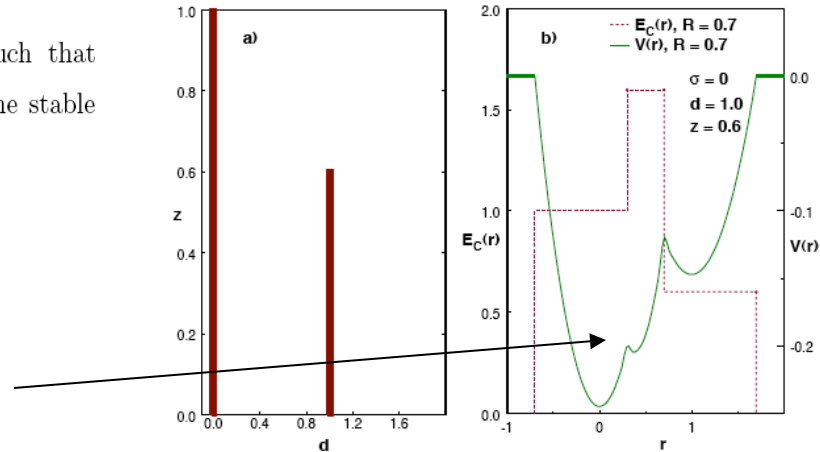
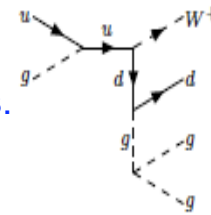


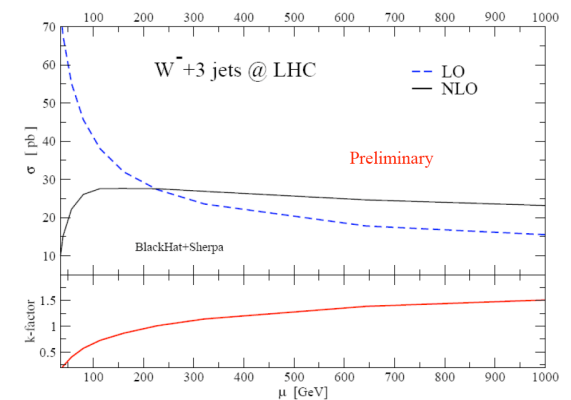
Figure 51. A schematic depiction of a specific parton configuration and the results of applying the midpoint cone jet clustering algorithm. The potential discussed in the text and the resulting energy in the jet are plotted.

Is the K-factor (at m_W) at the LHC surprising?

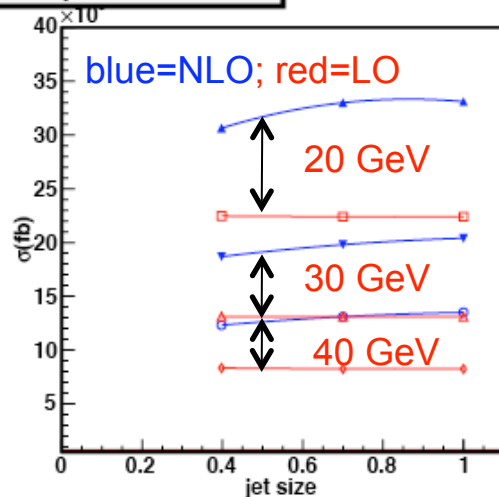
The problem is not the NLO cross section; that is well-behaved.
 The problem is that the LO cross section sits 'too-high'. The reason (one of them) for this is that we are 'too-close' to the collinear pole ($R=0.4$) leading to an enhancement of the LO cross section (double-enhancement if the gluon is soft (~ 20 GeV/c)). Note that at LO, the cross section increases with decreasing R ; at NLO it decreases. The collinear dependence gets stronger as n_{jet} increases. The K-factors for $W + 3$ jets would be more *normal* (>1) if a larger cone size and/or a larger jet p_T cutoff were used. But that's a LO problem; the best approach is to use the appropriate jet sizes/jet p_T 's for the analysis and understand the best scales to use at LO (matrix element + parton shower) to approximate the NLO calculation (as well as comparing directly to the NLO calculation).



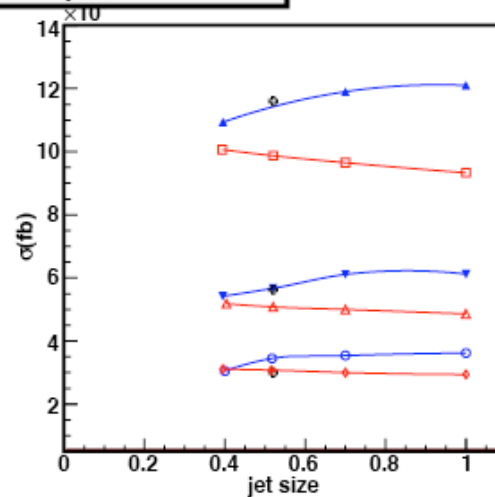
LHC total cross section



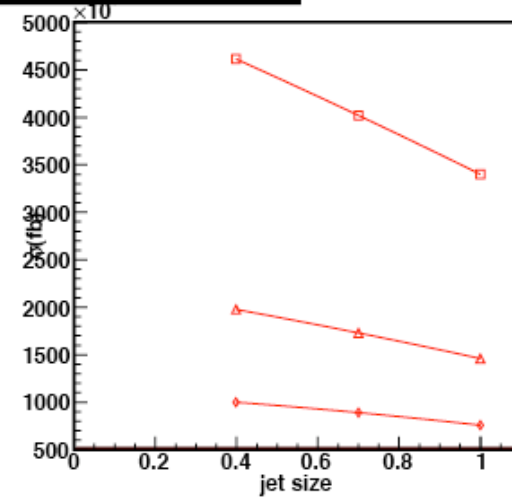
W + 1 jets cross section



W + 2 jets cross section



W + 3 jets cross section



For 3 jets, the LO collinear singularity effects are even more pronounced.

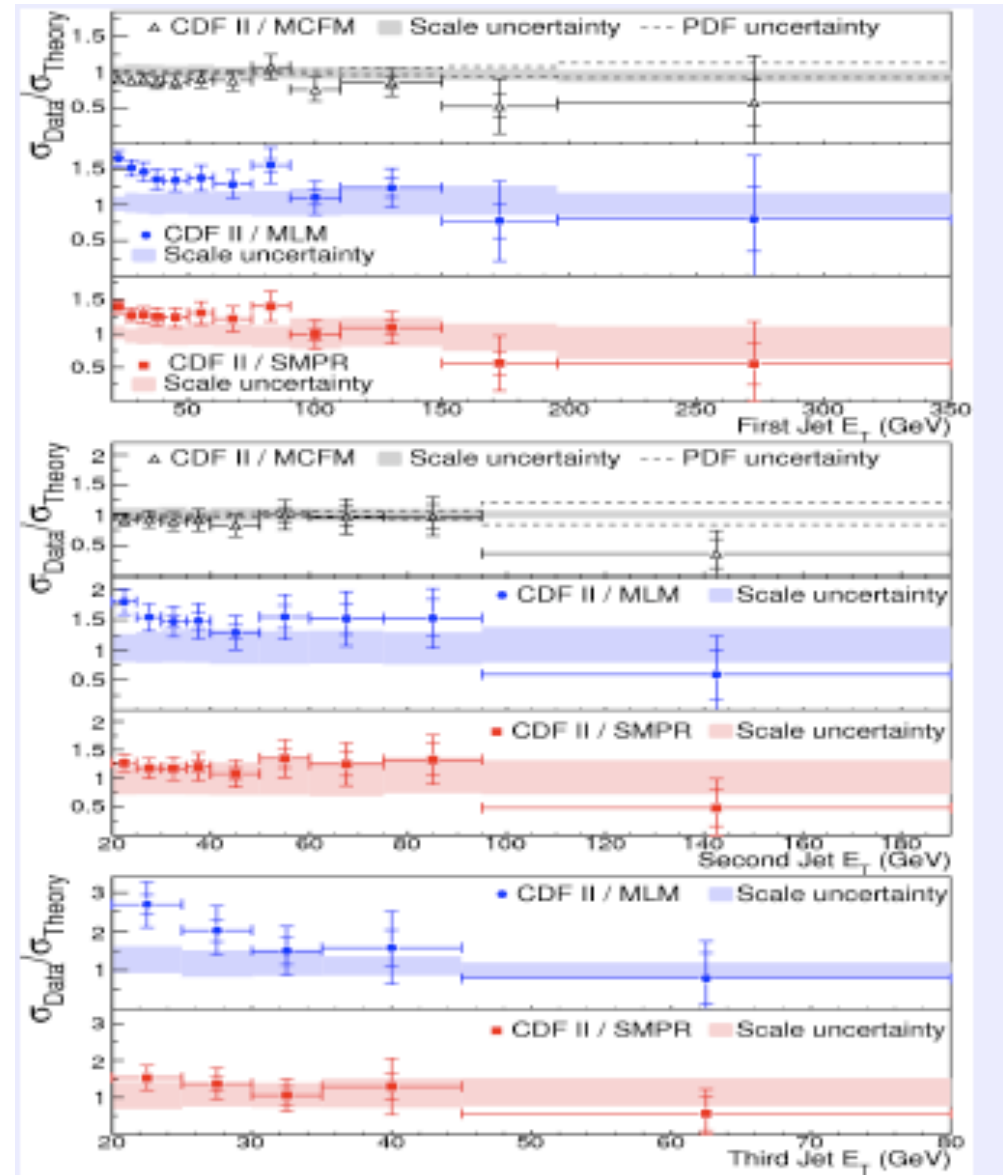
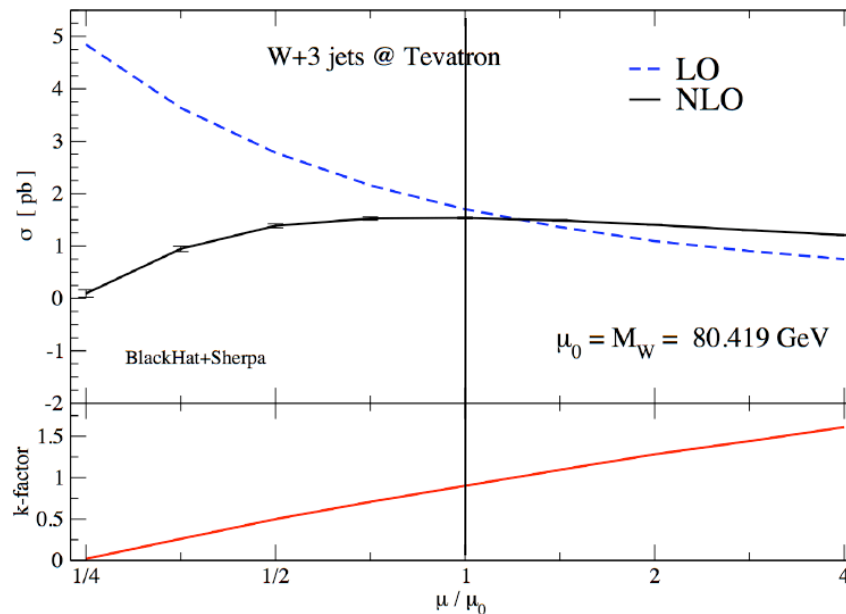
NB: here I have used CTEQ6.6 for both LO and NLO; CTEQ6L1 would shift LO curves up

Is this the end of the complications?

- We'll see later that additional complications are introduced by the fact that we don't measure partons in our jets in ATLAS, but energy that is distributed over a wide area of the detector by parton showering, hadronization and showering

W + jets at the Tevatron

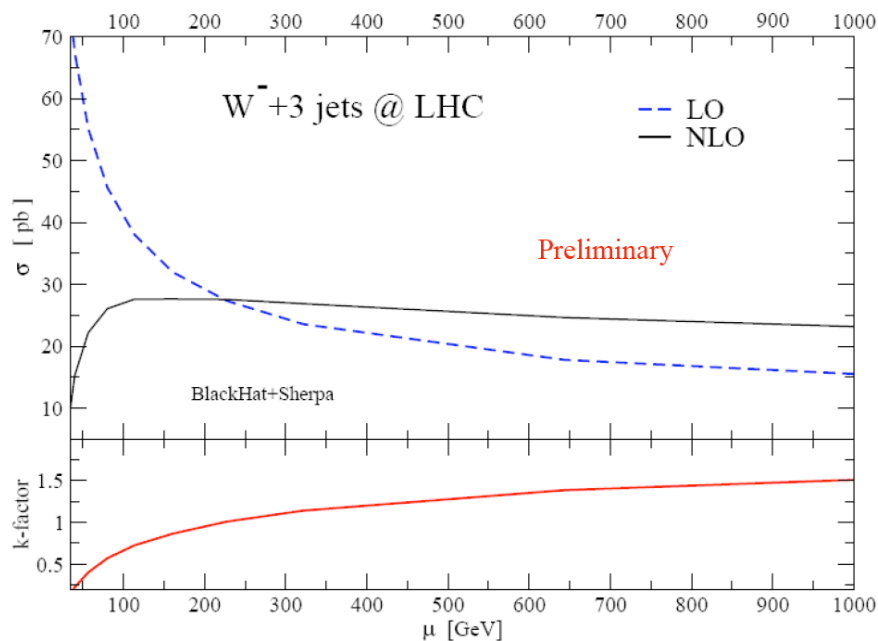
- At the Tevatron, m_W is a reasonable scale (in terms of K-factor~1)



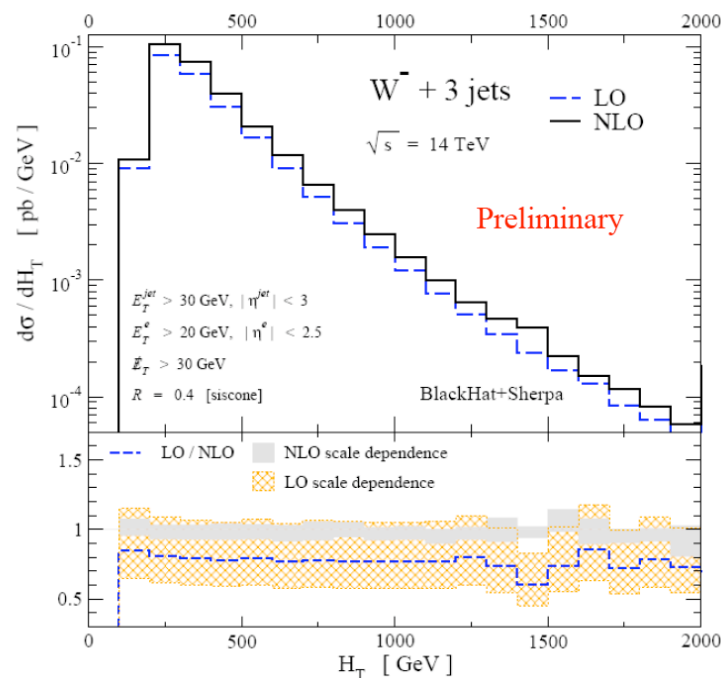
W + 3 jets at the LHC

A scale choice of m_W would be in a region where $LO \gg NLO$. In addition, such a scale choice (or related scale choice), leads to sizeable shape differences in the kinematic distributions. The Blackhat people found that a scale choice of H_T worked best to get a constant K-factor for all distributions that they looked at. Note that from the point-of-view of only NLO, all cross sections with scales above ~ 100 GeV seem reasonably stable. A CKKW-like scale also seems to work. Currently under investigation.

LHC total cross section



$$H_T = \sum_j E_{T,j}^{\text{jet}} + E_T^e + \cancel{E}_T \quad \text{distribution}$$



$$\mu = H_T$$

CKKW

- Applying a CKKW-like scale leads to better agreement for shapes of kinematic distributions

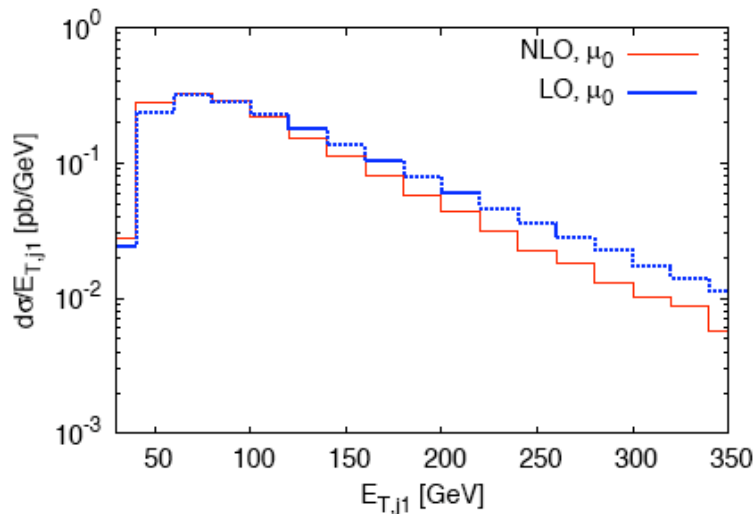


FIG. 3: The transverse momentum distribution of the leading jet for $W^+ + 3$ jet inclusive production cross section at the LHC. All cuts and parameters are described in the text. The leading color adjustment procedure is applied.

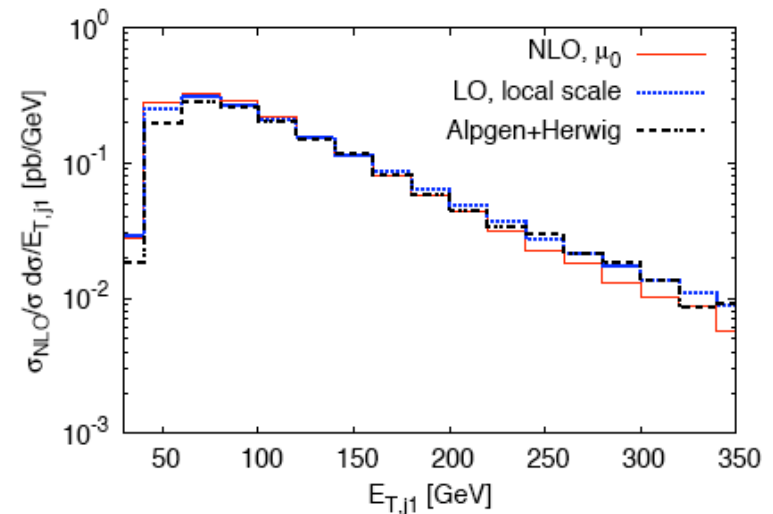


FIG. 4: The transverse momentum distribution of the leading jet for $W^+ + 3$ jet inclusive production cross section at the LHC. All cuts and parameters are described in the text. The leading color adjustment procedure is applied. All LO distributions are rescaled by constant factor, to ensure that the LO and NLO normalizations coincide.

See review of $W + 3$ jets in Les Houches
2009 NLM proceedings

0910.3671 Melnikov, Zanderighi

Choosing jet size

● Experimentally

- ◆ in complex final states, such as $W + n$ jets, it is useful to have jet sizes smaller so as to be able to resolve the n jet structure
- ◆ this can also reduce the impact of pileup/underlying event

● Theoretically

- ◆ hadronization effects become larger as R decreases
- ◆ for small R , the $\ln R$ perturbative terms referred to previously can become noticeable
- ◆ this restriction in the gluon phase space can affect the scale dependence, i.e. the scale uncertainty for an n -jet final state can depend on the jet size,
- ◆ ...under investigation

Another motivation for the use of multiple jet algorithms/parameters (i.e. SpartyJet) in LHC analyses.

Jet sizes and scale uncertainties: the Goldilocks theorem

- Take inclusive jet production at the LHC for transverse momenta of the order of 50 GeV
- Look at the theory uncertainty due to scale dependence as a function of jet size
- It appears to be a minimum for cone sizes of the order of 0.7
 - ◆ i.e. if you use a cone size of 0.4, there are residual uncancelled virtual effects
 - ◆ if you use a cone size of 1.0, you are adding too much tree level information with its intrinsically larger scale uncertainty
- This effect becomes smaller for jet p_T values on the order of 100 GeV/c
 - ◆ how does it translate for multi-parton final states?

Jet vetos and scale dependence: WWjet

- Often, we cut on the presence of an extra jet
- This can have the impact of improving the signal to background ratio
 - ◆ ...and it may appear that the scale dependence is improved
- However, in the cases I know about, the scale dependence was *anomalous* at NLO without the jet veto, indicating the presence of uncanceled logs
- The apparent improvement in scale dependence may be illusory

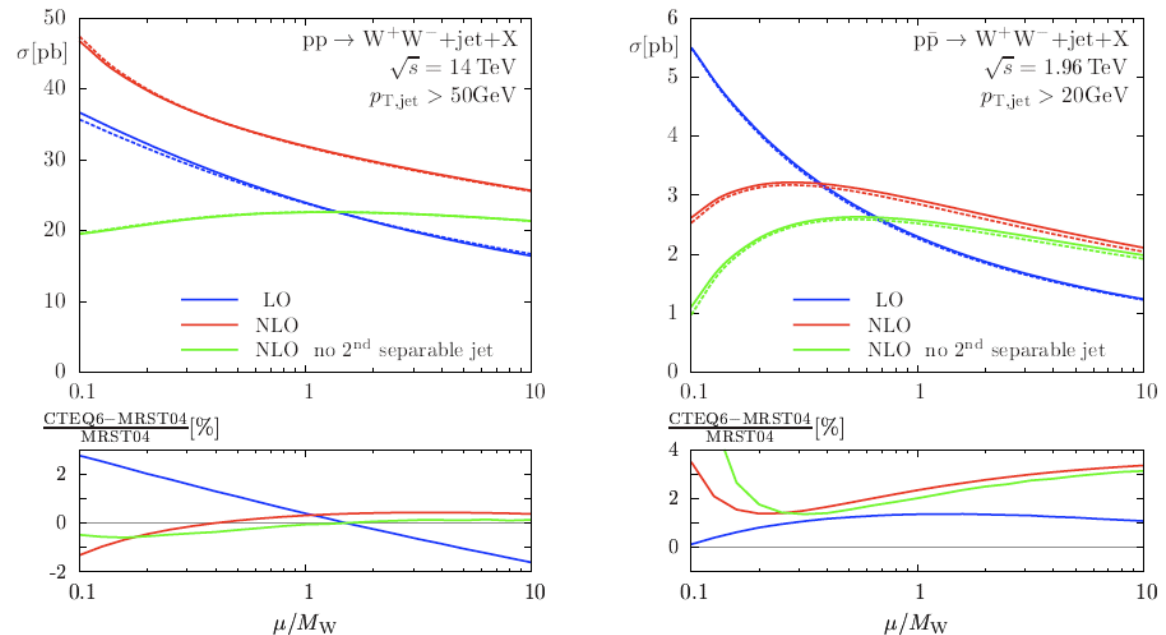
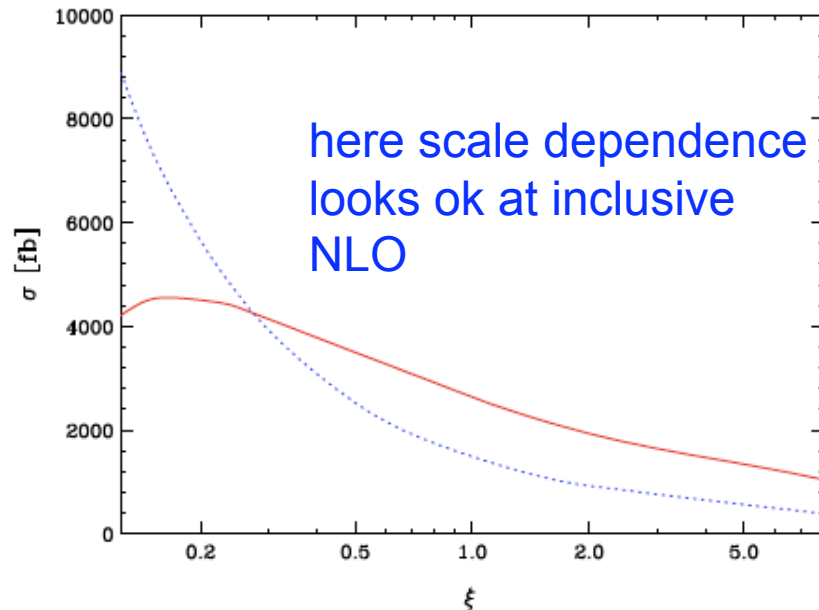


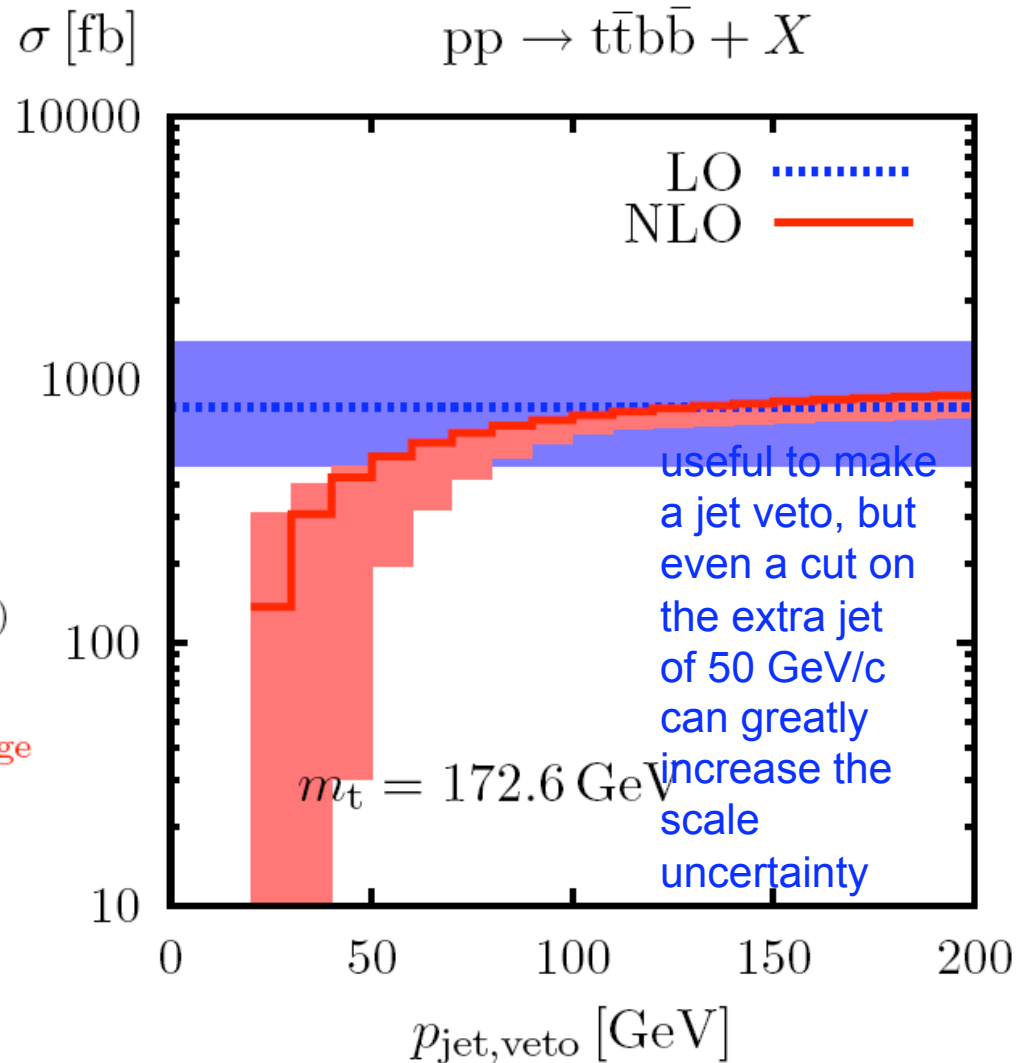
Figure 11: Comparison of WW+jet production cross sections in the LHC setup with $p_{T,\text{jet}} > 50 \text{ GeV}$ and for Tevatron with $p_{T,\text{jet}} > 20 \text{ GeV}$: The straight lines show the results calculated with the five-flavour PDFs of CTEQ6, the dashed lines those calculated with the four-flavour PDFs of MRST2004F4. Contributions from external bottom (anti-)quarks are omitted, as described in Section 2.2.

Consider tTbB



Perturbative instability for small $p_{\text{jet,veto}}$

- veto \Rightarrow negative contribution $-\alpha_s^5 \ln^2(Q_0/p_{\text{jet,veto}})$
- IR log dramatically enhances NLO uncertainty
- $p_{\text{jet,veto}} < 40 \text{ GeV} \Rightarrow$ **NLO-band enters $K < 0$ range**
NLO prediction completely unreliable!



Counter-example: $W + 3$ jets

- Here the NLO inclusive scale dependence looks ok
- Looks even better with exclusive cuts

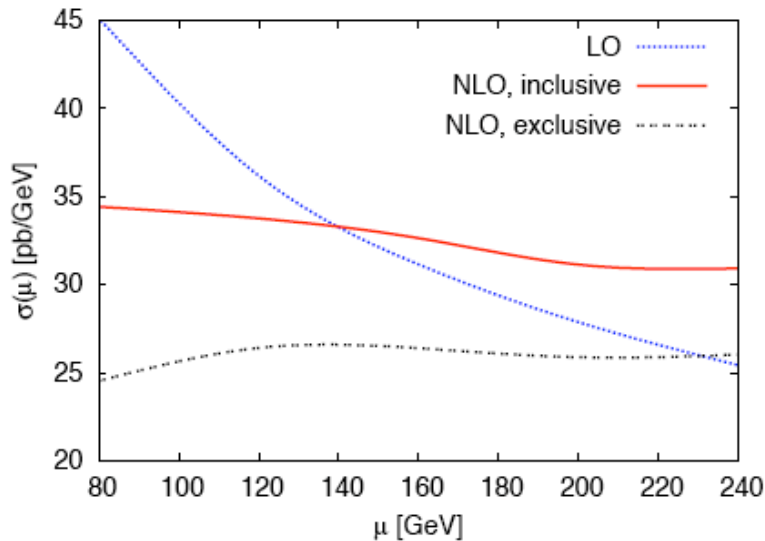


FIG. 1: The dependence of the $W^+ + 3$ jet inclusive production cross section at the LHC on the factorization and renormalization scale μ . All cuts and parameters are described in the text. The leading color adjustment procedure is applied.

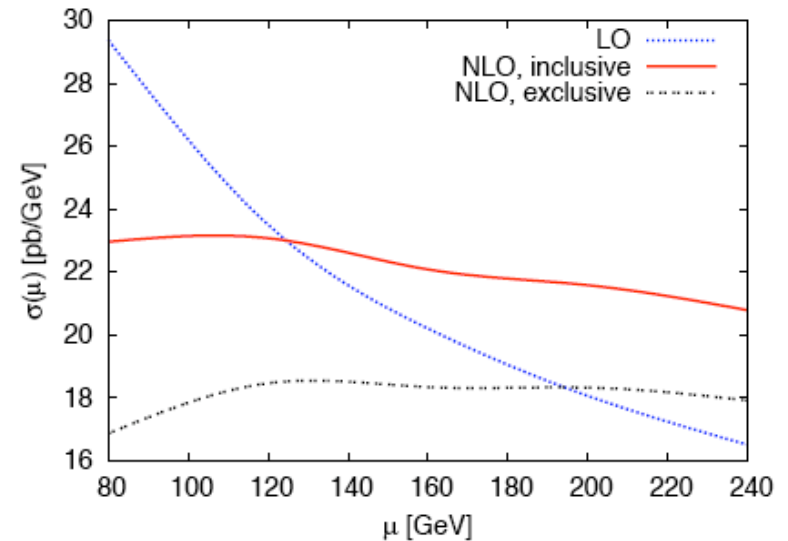


FIG. 2: The dependence of the $W^- + 3$ jet inclusive production cross section at the LHC on the factorization and renormalization scale μ . All cuts and parameters are described in the text. The leading color adjustment procedure is applied.

Jets at NLO continued

- Construct what is called a Snowmass potential

shown in Figure 50, where the towers unclustered into any jet are shaded black. A simple way of understanding these dark towers begins by defining a “Snowmass potential” in terms of the 2-dimensional vector $\vec{r} = (y, \phi)$ via

$$V(\vec{r}) = -\frac{1}{2} \sum_j p_{T,j} \left(R_{cone}^2 - (\vec{r}_j - \vec{r})^2 \right) \Theta \left(R_{cone}^2 - (\vec{r}_j - \vec{r})^2 \right). \quad (39)$$

The flow is then driven by the “force” $\vec{F}(\vec{r}) = -\vec{\nabla} V(\vec{r})$ which is thus given by,

$$\begin{aligned} \vec{F}(\vec{r}) &= \sum_j p_{T,j} (\vec{r}_j - \vec{r}) \Theta \left(R_{cone}^2 - (\vec{r}_j - \vec{r})^2 \right) \\ &= \left(\vec{r}_{C(\vec{r})} - \vec{r} \right) \sum_{j \in C(\vec{r})} p_{T,j}, \end{aligned} \quad (40)$$

where $\vec{r}_{C(\vec{r})} = (\bar{y}_{C(\vec{r})}, \bar{\phi}_{C(\vec{r})})$ and the sum runs over $j \in C(\vec{r})$ such that $\sqrt{(y_j - y)^2 + (\phi_j - \phi)^2} \leq R_{cone}$. As desired, this force pushes the cone to the stable cone position.

- The minima of the potential function indicates the positions of the stable cone solutions
 - the derivative of the potential function is the force that shows the direction of flow of the iterated cone
- The midpoint solution contains both partons

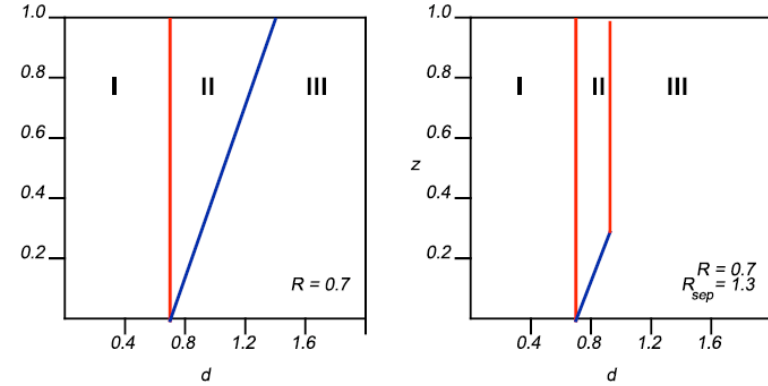


Figure 22. The parameter space (d, Z) for which two partons will be merged into a single jet.

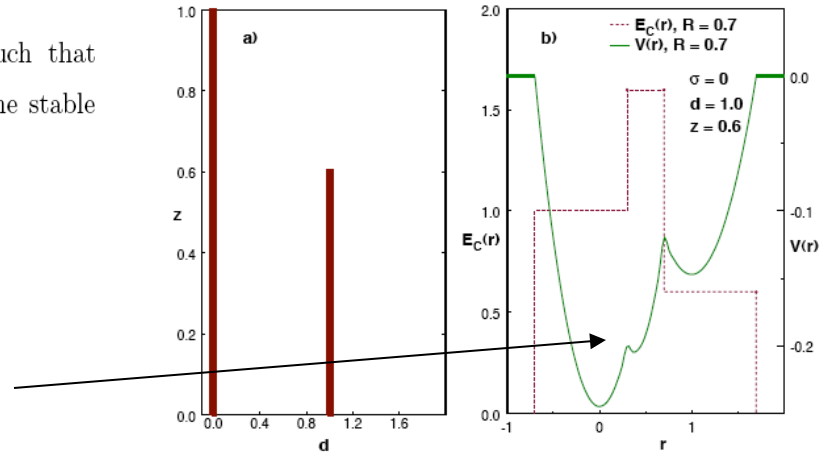


Figure 51. A schematic depiction of a specific parton configuration and the results of applying the midpoint cone jet clustering algorithm. The potential discussed in the text and the resulting energy in the jet are plotted.